॥ श्रद्धाहि परमा गतिः ॥

The National College Jayanagar

2 Day National Conference

CONDENSED MATTER AND SPACE SCIENCE

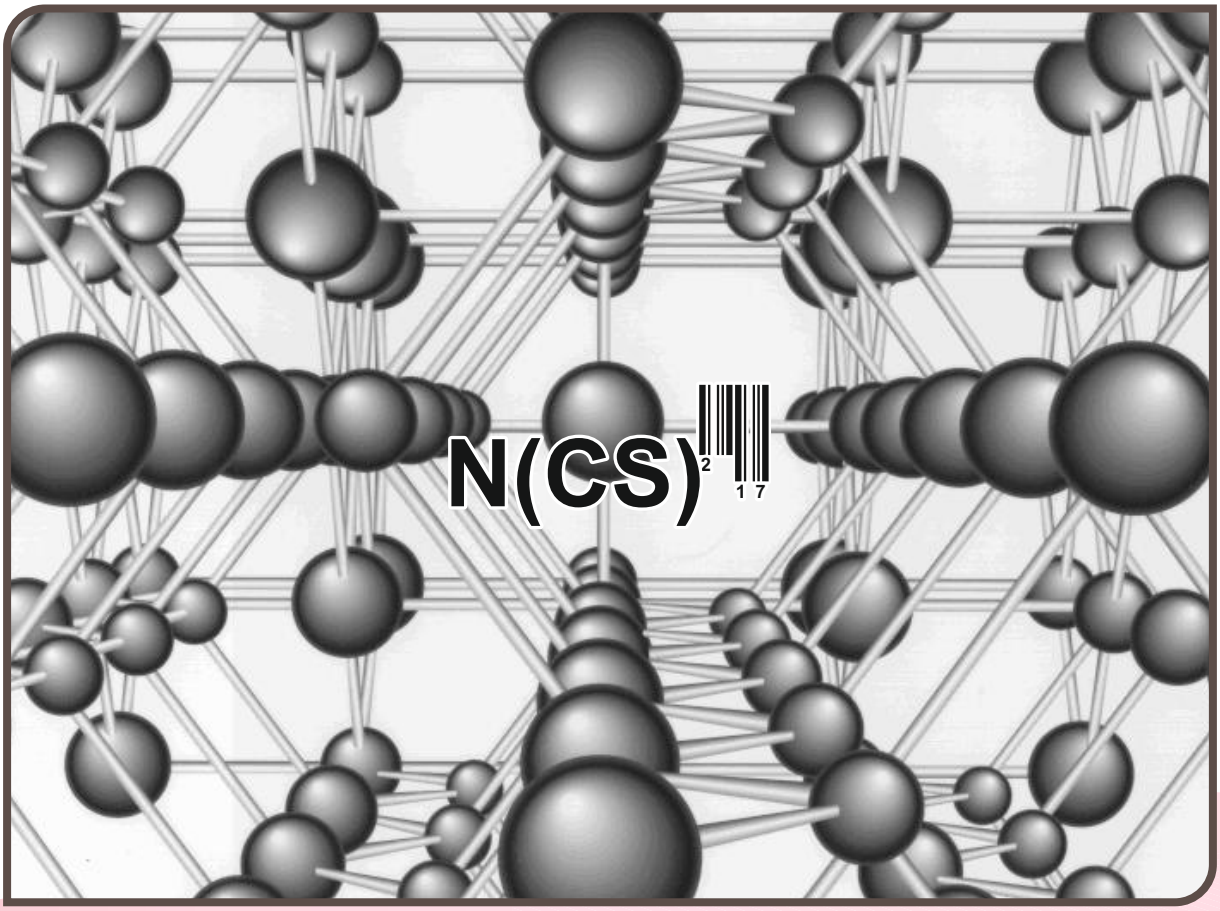

BOOK OF ABSTRACTS

ORGANIZED BY:

DEPARTMENT OF POST GRADUATE STUDIES AND RESEARCH IN PHYSICS

॥ ಶ್ರದ್ಧಾಹಿ ಪರಮಾ ಗತಿಃ ॥

Dr. A. H. Rama Rao

President,

The National Education Society of Karnataka,
The Bangalore Science Forum, Lalithakala
Parishath, Bangalore

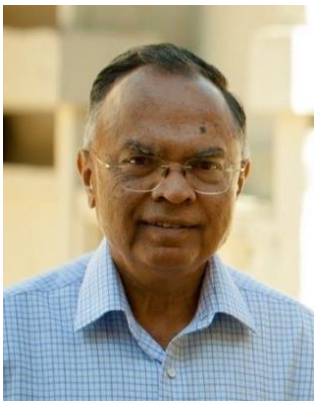

MESSAGE

The Department of Post Graduate Studies & Research in Physics of National College, Jayanagar is conducting the national conference on “Condensed Matter & Space Sciences" from 3rd July to 4th July 2015. This is highly commendable.

I am sure this conference would provide a great opportunity to all the students and teaching faculty to learn a great deal about the recent strides in optical and physical properties of rare-earth / metal nano-particles doped glasses and advances in space technology and the like.

Infact, P J Bhat, Distinguished Scientist (Retd), ISRO is giving us a keynote address on the topic "Recent development in satellite technology". This is in line with latest achievement of the space group of India.

All of us should support and encourage the team lead by Prof. R. Rajaramakrishna in conducting such conferences.

Dr. A .H. Rama Rao
President
National Educational Society
Bangalore

॥ ಶ್ರದ್ಧಾಹಿ ಪರಮಾ ಗತಿಃ ॥

Prof. S. N. Nagaraja Reddy

Hon. Secretary,

The National Education Society of Karnataka,
Bangalore.

MESSAGE

I am glad to learn that, The Department of Post Graduate Studies & Research in physics of our institution is organizing "2 Day National Conference on Condensed matter and space sciences" on 3rd and 4th of July 2017 for the benefit of students and delegates.

I send my compliments and best wishes to organizers, sponsors, delegates and all the aspirants of science for grand success of the event.

Prof. S. N. Nagaraja Reddy

(Secretary)

National Education Society

Bangalore

Dr. S. M. SHIVAPRASAD, PROFESSOR,
International Centre for Materials Science (ICMS)
Chemistry & Physics of Materials Unit (CPMU)
Jawaharlal Nehru Centre for Advanced Scientific Research (JNCASR)
Bengaluru - 560064
Email: smsprasad@jncasr.ac.in
Phone: 080-22082947

MESSAGE

I am very glad to learn that Department of PG Studies and Research in Physics, The National College, Jayanagar, is organizing a 2-Day National Conference on "Condensed Matter & Space Sciences" during July 3rd & 4th 2017 at Bangalore, involving invited lectures by subject experts, poster sessions and presentations. Organizing such events expose students and young researchers to the excitement that science offers. They become aware of contemporary developments, the scientific approach and also get access to meet subject experts to further their research interests. When I was young I found such conferences exciting to hear splendid talks and meet like-minded persons, which kept my fire of curiosity and eagerness to accomplish alive. I hope the youngsters participating in the conference will use this as an opportunity to identify the paths to tread so that they can further their interest in science. I congratulate the organizers for not only choosing a relevant topic for the conference but also leaving no stone unturned to make it useful and successful. I am looking forward to participate in the conference.

-SD

Dr. S. M. Shivaprasad
Professor
International Centre for Materials Science &
Chemistry & Physics of Materials Unit
JNCASR, Bengaluru.

Dr. C. K. JAYASHANKAR
PROFESSOR,
Department of Physics
Sri Venkateshwara University
Tirupati
Email: ckjaya@yahoo.com
Phone: 0877-2248033

MESSAGE

I am very glad to learn that Department of PG Studies and Research in Physics, The National College, Jayanagar, is organizing a 2-Day National Conference on "Condensed Matter & Space Sciences" during 3rd & 4th July 2017 at Bangalore, involving invited lectures by subject experts and poster/oral presentations by young researchers across the country.

I am sure that this will provide a platform for the participating delegates, research scholars and students to enhance their knowledge, understanding about the field and best part is to publish their research article. I also wish that this conference should be a grand success and pave the way to stimulate their contribution towards “MAKE INDIA”.

-SD

C.K. Jayashankar
PROFESSOR,
Department of Physics
Sri Venkateshwara University
Tirupati

Dr. B. Manikiam
Visiting Professor
Bangalore University

MESSAGE

I am indeed delighted to know that the prestigious The National College, Jayanagar is organizing a two day National Level Conference on "Condensed Matter & Space Sciences" during 3-4 July 2017. The topic of the Conference is highly relevant in the national and regional context and requires a multi-disciplinary approach of solution. The country being a mix of agrarian and industry based society has a large stake in climate change adaptation and needs to go in for environment based energy and development schemes. I hope that all aspects related to climate change impacts and measures will be deliberated in the Conference to arrive at appropriate solutions. I am glad to note that experts from the related fields are delivering special lectures which will motivate young faculty and students to take up research and career in this fast emerging field of Physics.

I wish the Conference all success.

Manikiam B

(Dr. B. Manikiam)

॥ ಶ್ರದ್ಧಾಹಿ ಪರಮಾ ಗತಿಃ ॥

Dr. H.R. Krishna Murthy

Principal,

The National College Jayanagar

Bangalore.

MESSAGE

I feel immensely happy that Post Graduate Department of Physics of our college is conducting a two day National conference on condensed matter and space sciences on 3rd and 4th July 2017.

The conference mainly focusses on recent development in the field of condensed matter and space sciences. The recent exploration and discovery of new materials have benefitted a lot in space science. It is in the connection the present conference assures importance.

I hope that this conference will bring together all the researchers, teachers and other new ideas on recent developments in space sciences. I wish this conference a grand success.

Dr. H. R. Krishnamurthy

(The Principal)

National College, Jayanagar

Bangalore

From,

The Editors Desk,

A thought that has been enduring in mind when it becomes real; is truly an interesting and exciting experience. The purpose of this conference is to introduce the participants in the new plethora of knowledge where every mind can share as a common platform, update their thoughts and emphasis their views in recent development of research activities. Department of PG Studies and Research in Physics, The National College, Jayangara, at Bangalore every year organizes conference for the student community to grow, share and update their research knowledge. Statement said by Anon "I hear, and I forget. I see, and I remember. I do, and I understand". This conference brings better understanding in the field of scientific research developments and provide a platform to every individuals to explore in science.

I have benefitted from the comments, advice and critics from many colleagues, who really want me to strive forward in administering the science activities to reach it to research scholars and student community.

I would show my deep respect to beloved professor Late. Sri. Dr. R. V. Anavekar for his extended support throughout his last minutes and dedicate this conference.

A great deal of emphasis on research projects for all the MSc students were made mandatory which has resulted them to prepare and present their research work in this conference. As the teaching faculty is highly motivated and dedicated to the students integral development a spontaneous and a huge response is found among the students to join this department.

I would like to thank Mr. J. Abhiram my student who really worked day and night and a backbone to the department who never say 'No' to any work which is assigned, Dr. Pramod who also helped me to bring this conference in a great event and Mr. B. P Siddalingeshwara, his driven energy which is profound and really would like to show my heartfelt thanks to these wonderful colleagues.

VISION:

Conference exists to unite, strengthen and inspire the leading academic scientists, researchers, research scholars and young minds to exchange and share their experiences and research results on all aspects of Condensed Matter Physics, Space Sciences. Conference will provide a unique integrated platform of workplace health and wellbeing in a professional and scientific arena ideal for hearing the latest science and viewpoints of research development activity.

MISSION:

To attract research scholars and students across the nation, and to contribute vigorously to their education and recent development in the field of research as responsible global citizens, future leaders of society, and leading practitioners of the basic sciences.

To offer advanced basic science and to incorporate the best pedagogical methods in its delivery during the period of conference.

To provide authors, research scholars, students with exceptional research and professional experience opportunities, support and guide them in their extracurricular pursuits, and challenge them to be proactive learners, deep thinkers and responsible citizens.

This is only a small step towards a long journey. To achieve progress and to meet objectives we have to cross numerous milestones. This conference should inspire all of us for a new beginning enlighten with hope, confidence and faith in each other in the road ahead.

Dr. R. Rajaramakrishna

Conference chairman,

NCCSS-2017

NCCSS -2017 Conference Schedule

Day 1: Monday, July 03rd, 2017

Time	Talk/Topic
10.30 AM- 12 PM	Inauguration – Mr. P. J. Bhat, Distinguished Scientist (Retd.), ISRO Keynote Address: Topic- Recent Developments in Satellite Technology
12-12.15 PM	High Tea + Poster Session 01
12.15- 1.30 PM	Dr. Shiva Prasad, JNCASR Topic- Nano manifestations of GaN thin films
1.30 PM-2.30 PM	Lunch
2.30-3.15 PM	Dr. Yellamggad, Centre for Soft Matter Research (CENS), Bangalore. Topic- Functional Organic materials for various device applications
3.15 – 3.30 PM	Tea + Poster Session 01
3.30-4.30 PM	Dr. Harish Barshilia, National Aerospace Laboratories (NAL), Bangalore. Topic- Thin film coatings for aerospace applications
4.30-4.45 PM	Poster Session 01
4.45 PM -5 PM	Visit to the PG department of Physics
5. 15 PM-6 PM	Cultural Event

NCCSS -2017 Conference Schedule

Day 2: Tuesday, July 04th, 2017

Time	Talk/Topic
10.30 AM-11.30 AM	Dr. Chandan Das Gupta, Indian Institute of Science, Bangalore. Topic- Glass transition in dense systems of self-propelled particles
11.30 AM-11.45 AM	High Tea + Poster session 02
11.45 AM-12.45 PM	Dr. B. Manikiam, Bangalore University Topic- Advances in Space Technology
12.45 PM-1.30 PM	Dr. B. Eraiah, Dept. of Physics, Bangalore University Topic- Free electron theory of metals
1.30 PM-2.30 PM	Lunch + Poster Session 02
2.30 PM-3.15 PM	Dr. Raghottama Rao, Former Scientist, DRDO. Topic- Testing and characterization of materials for space applications
3.15 PM-3.30 PM	Tea+ Poster Session 02
3.30- 4.15 PM	Dr. Chetan Rao, SDM College, Ujire Topic- Site specific transfer factors of radionuclides in Kaiga Region
4.15 PM-5 PM	Dr. Anand M. Y., Vijaya College, Bangalore Topic- Ultraviolet studies of interstellar bubbles
5 PM	Valedictory function + Award Ceremony for Poster presentations*

***Note:** Among all the posters presented, 03 Posters will be chosen for Best Poster Award.

Poster presentations:

Poster Session I **Day 1: 03rd July, 2017**	**P_01, P_02, P_03, P_04, P_05, P_07, P_09, C_05, C_06**
Poster Session II **Day 2: 04th July, 2017**	P_08, P_10, P_06, P_11, P_12, P_13, P_14, C_01, C_02, C_03, C_04

Index:

C_01: Optical and physical properties of Pr^{3+} doped Sodium Lead Calcium Borate glasses

C_02: Optical properties of Nd^{3+} doped BaF_2-ZnO-B_2O_3 oxyfluoride glasses

C_03: Study on capacitive type humidity sensors.

C_04: Urban Air electrical signatures at Gnana bharathi campus, Bengaluru (12.96°N, 77.5°E)

C-05: Quasi one-dimensional ZnO nano structures for efficient detection of hydrazine.

P_01: Stability of the anatase phase in nano dimensional TiO_2 doped with Eu^{3+}

P_02: Growth and characterization of Zn^{2+} mixed with cadmium oxalate crystals

P_03: Molecular confirmation and packing features in a series of aryl substituted tetra hydro pyrmidine-5-carboxylates.

P_04: Studying effect of carrier fluid viscosity in magnetite based ferro fluids using optical tweezers.

P_05: Long monitoring spectroscopic study of MRK 509 with IUE satellite

P_06: Nanosecond nonlinear optical properties of sodium triborate glasses doped with gold nanoparticles

P_07: A study on changing weather patterns in Bengaluru

P_08: Induced polystyrene effects on removal of natural polymer in Mangifera Indica.

P_09: Diurnal variations of atmospheric electric field at Mysuru (12 N, India).

P_10: Effect of Strontium on Li_2O-V_2O_5-B_2O_3 conducting glasses.

P_11: Chemical synthesis of Chromium oxide nano powders.

P_12: Crystal and molecular docking studies bis-cyclohexane diol with focal adhesion kinase inhibitors.

P_13: Physical and optical properties of copper doped Lanthanum Strontium borate glasses.

P_14: Effective electron densities and effective atomic numbers of brass solder lead and steel wool for gamma irradiation.

P_15: Growth and characterization of amorphous Nickel oxide thin films by SILAR method.

P_16: Energy and environment.

TABLE OF CONTENTS

Keynote Address

- Prof. P J BHAT 02

Invited Talk

- Dr S M SHIVAPRASAD 04
- Dr C V YELAMAGGAD 05
- DR HARISH C BARSHILIA 06
- DR CHANDAN DASGUPTA 07
- DR B MANIKIAM 08
- DR B ERAIAH 10
- DR P RAGHOTHAMA RAO 11
- DR CHETAN RAO 12
- DR M Y ANAND 14

Contributory Papers

- C_01 16-22
- C_02 23-36
- C_03 37-42
- C_04 43-51
- C_05 52-59

Poster Presentation

- P_01 - P_016 62-77

KEYNOTE ADDRESS

Recent Developments in Satellite Technology

P. J. Bhat,
Distinguished Scientist (Retd.), I.S.R.O

ABSTRACT

The period after Second World War witnessed severe competition between USA and Soviet Union in several domains, space technology being the prime among them. The launch of the first satellite – SPUTNIK in 1957 was the result of this space race. .Then onwards satellite technology has witnessed spectacular progress during the last six decades. Today, quite a few countries in the world have invested in development of satellite technology. Benefits of this field of science have been utilized in several domains of human life all over the world. Today, satellites in space play a pivotal role in communication, navigation, meteorology, remote sensing based applications and many other domains of day to day life of common man. Some of the man-made objects in space are also serving as effective tools for observation/study of celestial bodies and even for search for exoplanets and extra-terrestrial life. Satellites are providing support for many other areas of interest to individuals and countries also. In addition to major players like USA, Russia, China, Europe, India and Japan, some other countries and organisations have also focused on the development of satellite technology. With growing number of active satellites in orbit, the challenge posed by space junk created by nonactive satellites is also dictating the need for development of technologies for effective use of space domain in coming years. This talk deals with very recent developments in this area including the technological challenges expected in the coming few years.

INVITED TALK

IT_01: Nano-manifestations of GaN thin films

S.M. Shivaprasad
Jawaharlal Nehru Centre for Advanced Scientific Research, Bengaluru – 560 064, India
(smsprasad@jncasr.ac.in)

Recent developments in understanding the behavior of materials in low dimensions, has allowed synthesis of multi-functional materials. Advent of GaN and other wide band-gap semiconductors have revolutionized communication, solar energy harvesting and now in Solid State Lighting. We combine the band-gap engineering ability of the III- Nitrides and the novel manifestations of nano-materials, which display novel phenomena.

I will present our recent results of the growth and characterization of GaN thin films which has a unique Nanowall-Network morphology, grown on lattice mis-matched c-Sapphire substrate. The hexagonal self-assembled network is formed as open screw dislocations where the nanowalls are wedge shaped with the apex being less than a few nanometers and show confinement effects. I will show that this manifestation yields two orders of magnitude higher emission than conventional epilayers, due to its low defect density and a geometry that enhances light extraction. However, probing deeper we unravel that this non-centrosymmetric material supports Spontaneous Parameteric Down Conversion to emit a NIR light that escapes the nanowalls and accumulate in the void regions. Low temperature Cathodo-luminescence measurements results in a much enhanced laser-like, monochromatic emission in the NIR, due to Purcell effect.

The material also exhibits other very exciting properties. A combination of PL, Magneto-resistance, electrical measurements and quantum mechanical calculations establish that this system provides a novel route to the formation of a 2D-electron Gas in this system , enabling large electron mobility and coherence lengths. We also measure a localized spatial distribution of ferromagnetic domains at wall-apex, making it an interesting material for spintronics. Using this network as a template for lateral growth, we not only show very low defect GaN epilayer, but also Indium Nitride films and nanorods that display high quality with unprecedented electron mobility. Adsorption of Silver nano-clusters on the GaN nanowall network has shown further enhancement in light emission and this system serves exceedingly well as a very sensitive SERS substrate yielding unprecedented sensitivity for bio-molecular detection.

The morphology dependent multi-functionality and tunability by band engineering, make this unique system offer great scientific and technological promise.

IT_02 Functional Organic Materials for Various Device Applications

C. V. Yelamaggad*

Centre for Nano and Soft Matter Sciences

P.B. No. 1329, Prof. U.R.Rao Road Jalahalli, Bangalore 560013

Email: yelamaggad@cens.res.in

ABSTRACT

Functional materials have become the quintessential substances of the modern devices capable of supporting a wide range of new features. They are defined as novel chemical systems comprising functional organic and /or inorganic fragment(s) competent of portraying predestined properties. Indubitably, they constitute an important class of materials facilitating in-depth basic research and advanced cutting-edge technology developments. Although a broad range of substances fall under this category, some of the well-known, highly promising and performing materials include thermotropic and lyotropic liquid crystals (LCs), organogels, biomaterials, metal-ligand coordination polymers (COPs), metal-organic frameworks (MOFs), nanomaterials, conducting polymers, [13]organic-inorganic hybrid semiconductors, etc. In recent years there have been strategic efforts to develop an altogether different class of functional materials, called Nano-Soft Composites, where the nanoparticle (NP) and liquid crystal (LC) themes have been combined by realizing their hybrid (NP-LC) structures through bottom-up organic synthesis. Such NP-LC hybrids not only are fluids like those of liquids but also exhibit double refraction phenomenon as well as strong optical resonance arising from localized surface plasmon; these unique combined features are highly promising in photonics, sensors, photovoltaics, hyperlensing etc. Herein, we have designed, prepared and characterized several single-component gold NP-LC hybrids. The synthetic steps are extremely simple, hassel free and high yielding. Their full-structural elucidation has been carried out with the aid of standard spectroscopic methods, SEM/TEM imaging, AFM technique, EDX mapping and X-ray diffraction (XRD). The liquid crystallinity i.e., the fluid characteristics accompanied by birefringence of these hybrids has been evidenced with the aid of microscopic, calorimetric and XRD studies. The results of these investigations coupled with CD spectral data analysis confirm their self-organization in to new fluid chiral lamellar structures having handedness (chirality). In this presentation, I intend to discuss about this work; prior the basic aspects of functional materials and thermotropic LCs will be discussed.

IT_03: Thin film coatings for aerospace applications

Harish C. Barshilia

Surface Engineering Division
CSIR-National Aerospace Laboratories
HAL Airport Road, Kodihalli, Bangalore – 560 017
E-mail: harish@nal.res.in

ABSTRACT

There has been a lot of progress in the last decade or two on producing smaller/smarter devices with high performance. Nanostructured coatings and materials constitute a major area of scientific exploration and scientific pursuit in this development. Nanostructured materials, i.e., whose crystallites have dimensions of the order of few nanometers, exhibit extremely fascinating and useful properties. The unique properties of the nanostructured materials are due to small grain size, and consequent large volume fraction of atoms in or near the grain boundaries.

At CSIR-NAL, a large number of activities on nanoscience and nanotechnology are being pursued. The most significant amongst these are: Nanolayered/ nanocomposite coatings for tribological applications, supertough and solid lubricant coatings for high speed machining of difficult-to-machine materials, nanostructured coatings for renewable energy applications, nano-dimensional magnetic thin films for aerospace/engineering applications, superhydrophobic coatings for aerospace applications, carbon nanotubes and graphene for radar absorbing applications, transparent conductors for electronics and space applications. Research is also being carried out on the development of nanodots, nanopores, nanorods, nanotubes, etc. for improving magnetic, optical and electrical properties of a variety of electronic and optical materials. Attempts have been made to upscale the laboratory scale processes to indigenize these critical technologies for strategic sector. A summary of latest developments on these activities will be presented in this talk.

IT_04: Glass Transition in Dense Systems of Self-propelled Particles

Chandan Dasgupta

Department of Physics, Indian Institute of Science, Bangalore 560012, India

Investigations of the effects of activity or self-propulsion on the collective dynamics of soft glassy systems have received much attention in the last few years [1, 2]. This interest is driven in part by experiments on biological systems, such as bacterial cytoplasm [3], cytoskeleton-motor complexes [4, 5] and cell nuclei [6], in which chemical activity is found to fluidize a glassy state that exhibits characteristic glassy features such as caging, non-ergodicity and dynamical heterogeneity in the absence of activity. To develop a theoretical understanding of this activity-induced non-equilibrium glass transition, we have studied [7], using molecular dynamics (MD) simulations, the effects of active driving in a generic model glass former, the Kob-Andersen binary mixture [8]. Activity is introduced by assuming that a fraction $\rho_\alpha$of one kind of particles in the binary system experience a random active force f_0 that is correlated over a persistence timeτ_p.

Our main results are : (i) Tagged particle dynamics shows cage-hopping resulting in a late time diffusion coefficient that is weakly dependent on the temperature in the limit of large activity; (ii) Activity fluidizes the glass and dramatically reduces the glass transition temperature; (iii) The phase diagram in the (T-f_0) plane shows the complete disappearance of the glass phase beyond a threshold value of the activity; (iv) The effect of activity on dynamical correlation functions in the liquid state is determined by a specific combination of f_0, τ_p; and ρ_α that provides a measure of the relative magnitude of the "active" stress with respect to the stress arising from interparticle forces; (v) The presence of activity decreases the kinetic fragility of the liquid; and (vi) Activity leads to local clustering of the self-propelled particles induced by the passive particles in the glassy medium. We present simple analytic arguments, based on a heuristic Langevin description of the dynamics of a particle in the cage formed by its neighbors, which provide rationalizations of the shape of the phase boundary between fluid and glass phases in the (T-f_0) plane and other features observed in the dynamics of the system in the presence of activity.

This work was supported in part by CSIR (India), DST (India) and the Simons Centre and carried out in collaboration with Rituparno Mandal, Pranab Jyoti Bhuyan, Pinaki Chaudhury and Madan Rao.

[1] L. Berthier, Phys. Rev. Lett. **112**, 220602 (2014).

[2] R. Ni, M. A. C. Stuart and M. Dijkstra, Nat. Commun. **4**, 2704 (2013).

[3] Bradley R. Parry et al. Cell **156**, 1-12 (2014).

[4] N. Fakhri et al., Science, **344**, 1031 (2014).

[5] M. Guo et al., Cell **158,** 822 (2014).

[6] F. M. Hameed, M. Rao and G. V. Shivashankar, PLOS ONE **7**,10, e45843 (2012).

[7] R. Mandal, P. J. Bhuyan, M. Rao, C. Dasgupta, Soft Matter,**12**,6268, (2016).

[8] W. Kob and H. C. Andersen, Phys. Rev. Lett. **73**, 1376 (1994)

IT_05: Advances in Space Technology

B.Manikiam,

Bangalore University

Remote Sensing (RS)refers to the technology of acquiring information about the earth's surface (land and ocean) and atmosphere, using sensors onboard airborne (aircraft, balloons) or space-borne (satellites, space shuttles) platforms. The electromagnetic radiation is normally used as an information carrier in RS. Remote sensing employs passive and/or active sensors. Passive sensors are those which sense natural radiations, either reflected or emitted from the earth. On the other hand, the sensors which produce their own electromagnetic radiation are called active sensors (e.g. LIDAR, RADAR). Remote sensing can also be broadly classified as optical and microwave. In optical remote sensing, sensors detect solar radiation in the visible, near-, middle- and thermal-infrared wavelength regions, reflected/ scattered or emitted from the earth, forming images resembling photographs taken by a camera/sensor located high up in space.

Signature of any object and/or its condition comprises a set of observable characteristics, which directly or indirectly lead to the identification of an object and/or its condition. Computer aided techniques have been develop for interpreting satellite data.

Satellite Systems for Remote Sensing

The Earth Observation (EO) programme is basically applications- driven and development has been its prime motivation. Following the successful demonstration flights of initial satellites such as NOAA, TIROS in early 70s, development of unique satellite missions for earth observations was initiated. This led to operational satellites such as LANDSAT, SPOT, I.R.S with advanced sensors. The satellite data became a key provider of spatial information for natural resources management. Today we have satellites that can provide 1meter resolution data with high end applications such as urban development, infrastructure planning. It is interesting to trace the technology developments in the opto-electronic field and data transmission in the past decade.

Satellite data has become essential in several application areas such as agriculture, water resources, forestry and ecology, geology, watersheds, marine fisheries and coastal management. With the advent of high-resolution satellites new applications in the areas of urban sprawl, infrastructure planning and other large scale applications for mapping have been initiated. With the development of associated technology of GIS,

satellites are a tool for updating databases on resources.

RS application

Remote sensing observations provide data on earth's natural resources in a spatial format. The remote sensing (RS) data has the advantage of synoptic view and large area coverage. The information required in the field of civil engineering is derived mainly from analysis of image patterns present in the data. These patterns reflect the influence of the type of parent material, geological processes undergone, the climatic, biotic and physiographic environment and man's activity. Thus applications of remote sensing to engineering involve the recognition of basic landforms as indicated by the pattern elements on the image.

The satellite data has several applications in areas such as:

- Ground water mapping
- Agriculture crop inventorying
- Water management and Irrigation
- Urban planning
- Disaster management of Drought, Flood etc.
- Coastal management

Satellites have contributed significantly to weather forecasting through quantitativedata about the current state of the atmosphere and oceans. The chaotic nature of the atmosphere, the massive computational power required to solve the equations that describe the atmosphere, error involved in measuring the initial conditions so far contributed to less accurate forecasts. With meteorological satellites providing data and high power computation, the scenario has changed. Numerical weather prediction models run with large amount of weather observations provided by satellites and ground stations such as AWS, MBLM, GPS Sonde, Radar, LIDAR etc.

Future satellite missions are tuned towards watching the total earth system (land, water and atmosphere) and giving advance signals on climate changes.

IT_06: Free-electron theory of metals

Dr. B. Eraiah[*]

[*]*Department of Physics, Bangalore University, Bangalore - 560056*

[*]*eraiah@rediffmail.com*

ABSTRACT

The treatment of a metal as containing a cloud of electrons completely free to mve within it. The theory was originally proposed in 1900 to describe and correlate the electrical andthermal properties of metals. Later, quantum mechanicsbecame the basis for the theory of most of the general properties of simple metals such as sodium, with one free electron per atom, magnesium with two, and aluminum with three. Transition metals, such as iron, havepartially filled electronic *d* states and are not treated by the free-electron model.

Three years after J. J. Thomson's 1897 discovery of the electron, P. Drude suggested that thetransport properties of metalsmight be understood by assuming that their electrons are freeand in thermal equilibrium with their atoms.

This theory wasmade more quantitative byH. A. Lorentz. Assuming that themean free Path of electrons was limited by collisions, he was able to derive Ohm's law for the electrical Conductivity and obtain the ratio ofthermal toelectrical conductivityinexcellentagreementwith ex periment. This ratio is given by Wiedemann-Franz ratio and had been observed to be universal for over 50 years and counting.

IT_07: Testing and characterisation of materials for space application

S.Ramesh[1] and P. Raghothama Rao[2]

1. Former Scientist, I.S.R.O., Bengaluru.
2. Former Scientist, D.R.D.O., Bengaluru.

ABSTRACT

Materials form the backbone of any engineering system. A variety of materials are required to build any engineering system. The components required to work in the space environment must withstand all the expected environmental loads during its life time. In addition it is also required to demonstrate the design margins for each component. Material property plays an important part in the selection for the component. The material selected must be capable of withstanding presence of highly corrosive fluids, or fluids at very low temperature, high temperature, high pressure, acceleration etc during the flight.

Thus establishing of properties assumes immense significance in aerospace or similar hi-tech regime for the simple reason that safety and mission assume greatest importance. The study of engineering properties needs to be understood in the background of scientific phenomenon or premises. Thus characterization of materials refers to the unique and consistent properties of materials under the given condition. Testing forms the basis for characterization.

When one envisages application in space system, there cannot be better example for the highest reliability requirement perhaps next to medical or health regime. In this context it is to be reiterated that materials and components undergo wide fluctuation in the environment and that there is strong need to understand the behavior/performance of the materials under variety of stressing. For example a metallic material may fail in a brittle mode at a lower temperature while the same material reveals adequate or extended ductility at room temperature/elevated temperature. The presentation is intended to highlight the variety of tests to characterize the materials in space application with a few case studies.

IT_08: Studies on site-specific transfer factor for radionuclides in kaiga region

Chetan Rao

Dept. Of Post Graduate Studies and Research in Physics Sri Dharmasthala Manjunatheshwara College, Ujire - 574240

ABSTRACT

The paper presents a detailed study on site specific soil to rice plant and soil to vegetables (leafy, fruit and root) transfer factors for important radionuclides, such as, ^{210}Pb, ^{226}Ra, ^{228}Ra, ^{40}K, and ^{137}Cs for Kaiga region, India where four pressurised heavy water reactor (PHWR)**,** each of 220 MW (e) generating capacity**,** are operating. An experimental rice and vegetable fields were developed at about 500 m aerial distance from the Nuclear Power Plant (NPP) site at Kaiga to study the site-specific soil to plant transfer factors. Paddy and different types of vegetables were grown in the experimental field, during different seasons of the year, using the discharge water from the Kaiga nuclear power plant. For a comparative study of the transfer factors obtained for the experimental field, samples were also collected from the identified nearby villages**.**Samples of rice and vegetables grown in the experimental field using discharge water of NPP and by the local farmers using normal water resources were collected and analyzed. The transfer factors were estimated for important radionuclides, such as, ^{210}Pb, ^{226}Ra, ^{228}Ra, ^{40}K, and ^{137}Cs**.** The analysis of the radionuclide concentrations were carried by gamma spectrometry method using High Pure Germanium gamma spectrometer (HPGe). More than 600 transfer factor values were estimated for the above mentioned radionuclides and stable elements.

The mean values of soil to rice grain transfer factors for ^{40}K, ^{210}Pb, and ^{137}C were 1.4, 1.5×10^{-1}, and 2.1×10^{-1}, respectively. Similarly soil to plant transfer factors for different types of vegetables (leafy, fruit and root) are discussed and presented. The mean values of transfer factors of ^{210}Pb, ^{226}Ra, ^{228}Ra and ^{137}Cs observed in the present study for rice and different vegetables were comparable to the values compiled in IAEA, TRS-472 (2010) and other literatures, whereas, the transfer factor values for ^{40}K were an order of magnitude higher.

The $^{137}Cs/^{40}K$ discrimination factors were evaluated and were generally less than unity. The correlation analysis between ^{137}Cs transfer factors and ^{137}Cs to ^{40}K discrimination factors for different organs of the rice plant yielded significant positive correlation coefficients. The annual effective dose due to intake of rice by the population of Kaiga from ^{40}K was found to be in the range of 15.5 – 50.2 μSv $a^{-1}$with a mean value of 26.6 μSv a^{-1}. The AED from ^{210}Pb was in the range of 4.6 – 56.2 μSv $a^{-1}$with a mean value of 19.4 μSv a^{-1}, and AED from ^{137}Cs varied in the range of 0.05 – 1.5 μSv $a^{-1}$with a mean value of 0.66 μSv a^{-1}. The annual dose to the population (an adult member) of Kaiga from ^{210}Pb, ^{226}Ra, ^{228}Ra, ^{40}K, and ^{137}Cs due to consumption of all types of vegetables, was estimated to be 793.0 μSv a^{-1}. Effort was made to verify the assumption that the transfer factor for a radionuclide or an element is constant regardless of the element concentration in the soil. It was found that radionuclide concentration in rice and vegetable plants are not linearly related to soil concentration. Also, the study did not reveal any significant correlation coefficients between the physico-chemical properties of the soil and the radionuclide transfer factors to above the ground organs. The study has also shown that continued use of the discharge water in the experimental rice field has not resulted in the increase of the ^{137}Cs activity concentration in the soil of the rice and vegetable fields which suggests no radiological impact of the nuclear power plant on the main food cultivation of the region.

IT_09 : Ultra violet studies of interstellar bubbles

Dr. M Y Anand

Department of P.G. Physics, Vijaya College, Bangalore

ABSTRACT

In this talk, I will discuss about the need and techniques of Ultraviolet studies of interstellar medium in general and interstellar Bubbles in particular. Initially interstellar medium is named after the matter between the stars, now all the gas (atomic/molecular) and dust in a galaxy is termed as interstellar matter. Spectroscopic studies of these interstellar matter reveals much information about the physical condition of these matters and many important diagnostic matters fall in the UV region, hence UV studies of these interstellar matters become very important. Massive hot stars in the interstellar medium form interstellar bubbles because of the interaction of stellar winds (or supernovae) with the interstellar medium. With reference to few interstellar bubbles methodology of spectral analysis will be discussed and brief introduction to Ultraviolet telescope like IUE, FUSE etc., will be given to understand how UV astronomy is done.

CONTRIBUTORY PAPERS

C_01: Optical and Physical properties of Pr^{3+} doped sodium lead calcium borate glasses.

Susheela K. Lenkennavar[1,2], Madhu. A[1], B. Eraiah[1], M.K. Kokila[1]*

[1]Department of physics, Bangalore University, Bangalore -56, India

[1,2]Dept of physics, FMKMC College, Constituent College of Mangalore University, Madikeri-571201, Karnataka, India

E-mail: drmkkokila@gmail.com

Abstract: This paper reports Pr^{3+} doped sodium lead calcium borate glass preparation. The present glasses were prepared using melt quenching technique quenched at 1030^0C. With varied concentration of Pr^{3+} the impact on optical and physical properties of the glasses have been examined.The X-Ray diffraction analysis of the prepared samples confirms the amorphous nature of the glass samples. Few physical parameters of the glasses like refractive index(n), density (ρ), molar volume (V_m), molar refractivity (R_m), polarizabilities (α_m), concentration of rare earth ion (N_i) , polaron radius (r_p) , inter ionic distance (r_i), field strength(F), reflection loss (R_L%) and dielectric constant (ε) energy band gap and urbach energy are calculated and tabulated.

Keywords: Alkaline Borate Glass, X RD, Optical absorption spectra

1. Introduction

Rare-earth ions doped lead oxide based glasses have been prepared and characterized to understand their commercial applications as the glass lasers and also in the production of wide variety of other types of optical components. The pure borate glasses possess low refractive index, high melting point and high phonon energies in the order of 1300–1500cm^{-1}. There are some alkali borate glasses reports. It is assumed that in such glasses each alkali oxide associates with a proportional quantity of B_2O_3. The number of BO_3 and BO_4 units related to each type of alkali oxide depends on the total concentration of alkali oxide. It is concluded that in mixed alkali borate glasses the volumes of structural units related to an alkali ion are the same as in the corresponding binary alkali borate glass. This reveals that each type of alkali oxide forms its own borate matrix and behaves as if not affected with the presence of the other alkali oxide[1].Praseodymium doped glasses find variety of practical applications such as UV-VIS-NIR lasers, up-converters , optical fiber lasers , fiber amplifiers in 1.3 μm region [2,3,4,5] etc. These applications can either be enhanced or optimized from systematic study of optical properties of Pr^{3+}ions in various environments. In the present work we are concentrating on Pr^{3+} ions doped in sodium lead calcium borate glasses. Optical behavior of these glasses are carried out to know the effect of rare earth ion in alkali borate glass also to observe the defects created when the Pr^{3+} ions doped into it.

2. Theory

The absorption coefficient α (υ), in amorphous materials, in the optical region near the absorption edge at particular temperature, obeys empirical relation known as, Urbach rule [6] given by

$\alpha(\vartheta) = \alpha_0 \exp(h\vartheta/E_U)$ ..... (1)

Where, hυ is photon energy, α_0 is a constant and E_U is an energy which interpreted as the width of the localized state in the normally forbidden band gap which is also known as the Urbach energy. Optical absorption in solids and liquids occur by various mechanisms in all of which the photon energy will be absorbed by either lattice or by electrons where the transferred energy is conserved. The lattice (or phonon) absorption will give information about the atomic vibration involved and this absorption of radiation normally occurs in the infrared region of the spectrum. The higher energy parts of the spectrum particularly those associated with the interband electronic transition will provide further information about the electron states. In these processes, the electrons are excited from a filled band to an empty band by the photon absorption and as a consequence of this, a marked increase in the absorption coefficient α (υ), will result. The onset of this rapid change in a(υ) is called the 'fundamental absorption edge' and the corresponding energy is defined as the 'energy gap' [7].In amorphous materials the absorption due to the band-to-band transitions that determines the optical energy gap was interpreted by Davis and Mott [8]and can be written in general form:

$$\alpha(\vartheta) = (B/h\vartheta)(h\vartheta - E_{opt})^n \text{..... (2)}$$

Where, B is a constant and hυ the photon energy, E_{opt} the optical energy gap and n is an index which can have any values between 1/2 and three depending on the nature of the interband electronic transitions [9].The goodness of the fit of the data to the formula for either n = 1/2 (direct band gap) or n = 2 (indirect band gap) is determined. It has been found that [9-13] for many amorphous materials, a reasonable fit of Eq. (2) with n = 2 are achieved. This is the case of indirect transitions, where the interactions with lattice vibrations take place.

3. Experimental

The samples Pr^{3+} doped sodium lead calcium borate glass, ($(20Na_2O$ -10PbO-10CaO -$60B_2O_3$-xPr_2O_3) (where, x=0, 0.1, 0.3, 0.5mol% of Pr^{3+}) is here after named as NPCB, NPCB01, NPCB03, NPCB05 were prepared by melt quenching method. The mixture of analytical grade of sodium carbonate, lead oxide, calcium carbonate, boric acid and praseodymium trioxide (99.99%) were mixed homogeneously in agate and motor for 30 minutes. The batch was melted in porcelain crucible at 1000-1080^{0}C for 30 minutes (stirred for homogeneous mixing) and quickly poured on a preheated brass moulds to get pellet form samples which were polished for few analysis. The glassy nature of samples was confirmed by XRD measurements (Rigaku Ultima IV) using Cu-Ka radiations (λ = 1.54 Å) with copper filters operating at 40 kV and 100 mA. The 2θ range was 0^0–80^0 with step size of 0.2^0 and are solution of 0.01^0. The optical absorption spectra of polished samples have been recorded at room temperature in the wavelength range 400nm - 800nm using Pekin Elmer lambda-35 UV-Vis spectrometer. Few physical parameters like refractive index and density were also calculated. The densities (ρ) of the glass samples were measured using Archimede's principle with toluene as an immersion liquid. Refractive indices (n)

of samples were measured at 589.3 nm (sodium wavelength) using an Abbe's refractometer (Model CL: 1.30-1.71) with monobromonaphthalene as the contact liquid.

4. Results and Discussion

4.1 Physical parameters.

The refractive index of the present glass matrix is higher (~1.62). The observed results of glasses express that density and molar volume both are following the trend as expected .As the density decreases, the molar volume will increase[14]. It's also observed in the Fig.[1]. As the concentration increased the inter-ionic distance decreases which results in increase in field strength of Pr^{3+} ion in the host matrix. This variation in the inter-ionic and field strength is clearly represented in Fig.[2].

Physical parameters of the glasses like Refractive index(n), density (ρ),Molecular weight(M.W), molar volume (V_m), molar refractivity (R_m), polarizabilities (α_m), concentration of Rare earth ion (N_i) , polaronradius (r_p) , inter ionic distance (r_i), Field strength(F), Reflection loss (R_L%) and Dielectric constant (ε) are calculated and reported in the Table 1.

Glass	n	ρ(g/cm^3)	M.W(g)	V_m (cm^3)	R_m (cm^{-3})	α_m (×10^-24)cm^3	N_i(×10^20) ions/cm^3	r_p (nm)	r_i (nm)	F (×10^15) cm^{-2}	R_L(%)	ε
NPCB	1.624	3.36	82.498	24.55	8.666	3.431	-	-	-	-	5.656	2.637
NPCB01	1.628	3.06	82.425	26.93	9.563	3.786	0.446	1.832	2.862	0.893	5.717	2.652
NPCB03	1.626	3.404	83.085	24.40	8.634	3.419	1.470	1.231	1.924	1.979	5.682	2.643
NPCB05	1.627	3.308	83.744	25.31	8.970	3.552	2.367	1.051	1.642	2.719	5.697	2.647

Table.1. Physical parameters of Pr^{3+} doped NPCB glasses

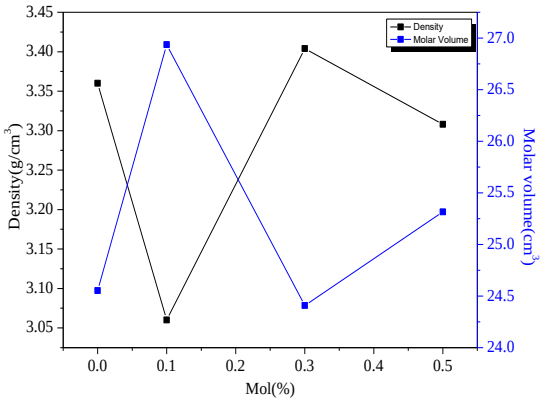

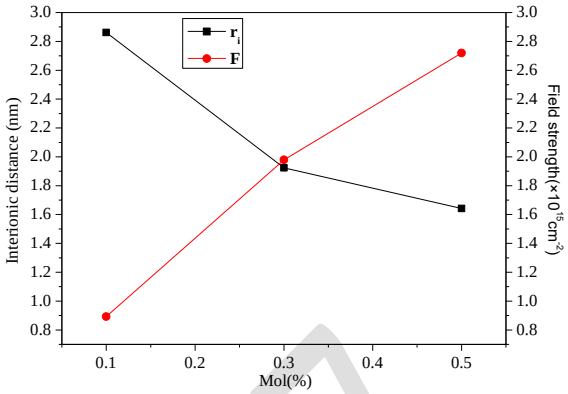

Fig.1.Density v/s molar volume of the glasses.

Fig.2. Inter ionic distance v/s Field strength of the glasses.

4.2 **.Structural properties**

The typical X-ray diffraction pattern of the glasses is shown in figure 3 and in which the presence of a broad hump between 40^0 and 50^0 without any sharp crystallization peak confirms the amorphous nature of the samples. The XRD features of all samples are nearly the same.

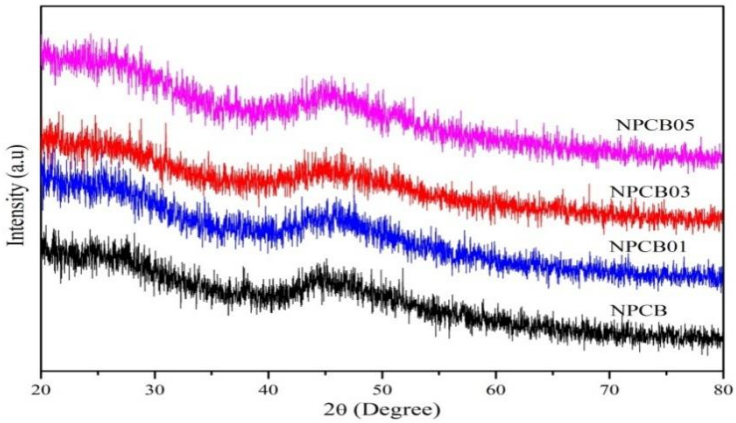

Figure 3: XRD patterns of glass samples doped with different concentration of Pr^{3+}.

4.3. Optical absorption spectra

The optical absorption coefficient α(υ), was calculated for each sample at different photon energies by using the relation α(υ)= A/d, where A is the absorbance and d is the thickness of the samples. The spectra in visible region are as shown in Fig.4. For Pr^{3+} doped NPCB glasses. We can clearly observe inhomogeneous prominent 4 peaks due to 4f transitions of Pr^{3+}ions. The 4 peaks at 443nm, 470nm, 482nm and 592nm are due to $^3P_2$, $^3P_1$, $^3P_0$ and $^1D_2$ respectively from $^3H_4$ ground state of Pr^{3+}ions. As the Pr^{3+} ions are increased the intensity of the peak also increasing of NPCB glasses. Using equation (1&2) direct, indirect band gap and urbach energy is calculated as shown in Fig.5 and 6. Direct(E_D) and indirect band gap (E_{In}) shows decreasing in nature as

concentration of Pr^{3+} ions is increased in NPCB glasses. This suggests that the non-bridging oxygen ion content increases with increasing Pr_2O_3 content and there by shifts the band edge to lower energies and in-turn lead to have a decrease in the E_{opt} values. E_D and E_{In} values are varied from 2.93eV -2.04eV and 2.9eV to 1.34eV respectively. From the equation (1), the exponential behavior is observed due to the band tails associated with the valence and conduction bands which extend into the band gap [15,16]. The magnitude of the Urbach energy (E_U) the width of localized states can be used to characterize the degree of disorderness in the amorphous / crystalline materials. Materials with larger Urbach energy would have greater tendency to convert weak bonds into defects. The E_U is found to be 0.31eV -1.66eV from the Fig 7. , therefore weak bonds is converted into defects as Pr^{3+} ions concentration is increased. While increasing the Pr_2O_3 content in the host matrix, the non-bridging oxygen ion content increases there by shifting the band edge to lower energies, which in-turn decreases the optical band gap energy values and increases the Urbach energy values[17,18]. Values of E_D, E_{In} and E_U each Pr^{3+} of NPCB glasses are reported in Table.2.

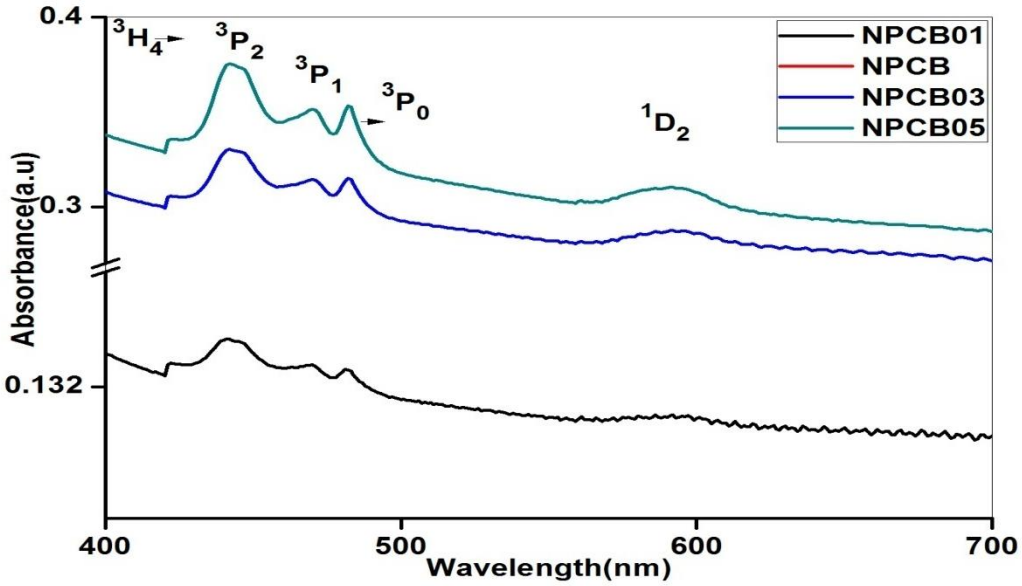

Fig.4. Absorption spectra in visible region of NPCB glasses.

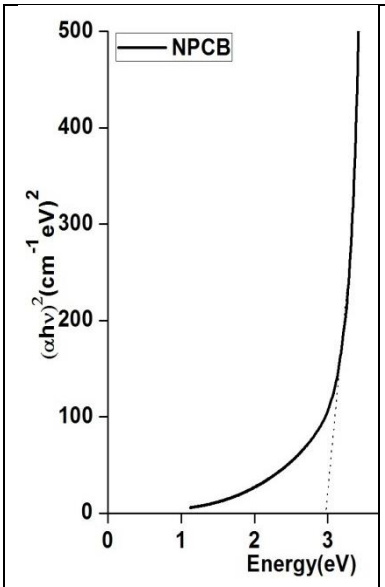

Fig.5.Direct energy band gap

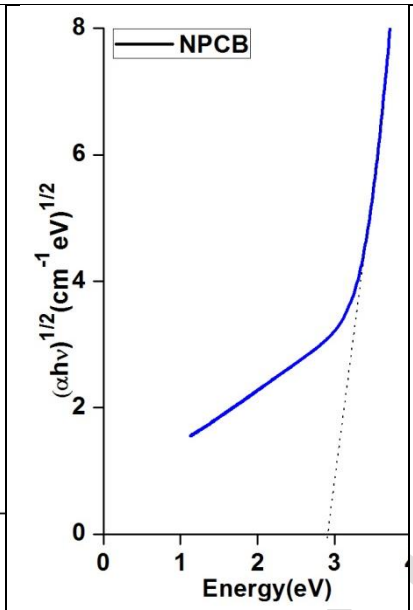

Fig.6. Indirect energy band gap

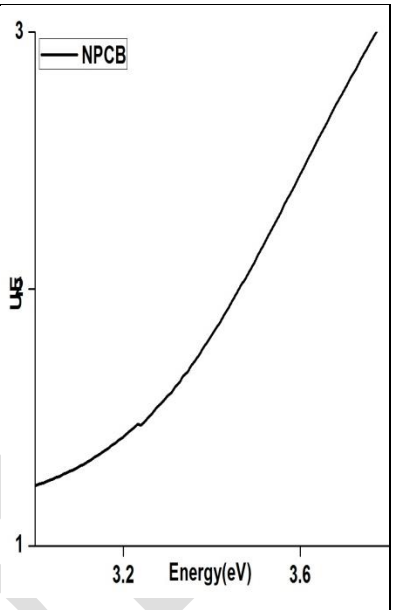

Fig.7. Urbach energy

Table 2: Optical Properties of glasses at different concentration of Pr^{3+}			
Glasses	Direct band gap energy, **E_D(eV)**	Indirect band gap energy, **E_{In}(eV)**	Urbach energy, **E_U(eV)**
NPCB	**2.93**	**2.9**	**0.31**
NPCB01	**3.13**	**2.16**	**0.9**
NPCB03	**2.29**	**1.63**	**1.35**
NPCB05	**2.04**	**1.34**	**1.66**

5. Conclusions

In the present work, Pr^{3+} doped NPCB glasses optical properties were analyzed and few physical properties are also calculated. We can observe the 4 transition peaks of Pr^{3+} ions in NPCB glasses in UV-Vis region have increasing intensity of peaks as the concentration is increased. The Tau's plot results the direct and indirect band gap to be decreased as the concentration of Pr^{3+} ions is increased which concludes that the non-bridging oxygen ion content increases with increasing Pr_2O_3 content and there by shifts the band edge to lower energies and in-turn lead to have a decrease in the E_{opt} values. These glasses have increase in Urbach energy therefore weak bonds are converted into defects as Pr^{3+} ions concentration is increased. Few physical parameters like density, molar volume ,molar polarizbility and RI are also reported.

6. References

1. H. Doweidar , G.M. El-Damrawi, Y.M. Moustafa, R.M. Ramadan,,Physica B, Volume 362, Issues 1–4, 15 May 2005, 123–132

2. A.A. Kaminskii, Laser Crystals, 2nd Edition, Springer,Berlin, 1990.
3. D.B. Gatch, S.A. Holmstrom, W.M. Yen, J. Lumin. 83}84(1999) 55.
4. D.M. Baney, L. Yang, J. Ratcli!, K.W. Chang, Electron.Lett. 31 (1995) 1842.
5. Y. Zhao, S. Fleming, IEEE J. Quant. Electron. 33 (1997)905.
6. F. Urbach, Phys. Rev. 92 (1953) 1324.
7. C.A. Hogarth, A.A. Hosseini, J. Mater. Sci. 18 (1983) 2697.
8. N.F. Mott, E.A. Davis, Philos. Mag. 28 (1970) 903.
9. S.K.J. Al-Ani, A.A. Higazy, J. Mater. Sci. 26 (1991) 3670.
10. A.A. Higazy, M.A. Hussein, M. Ewaida, M. Elhoft, J. Mater. Sci.Lett. 7 (1988) 453.
11. A.A. Higazy, M.A. Hussein, M. Ewaida, J. Mater. Sci. Lett. 24 (1989)2203.
12. A.A. Higazy, B.Y. El-Baradic, M.I. Abd El-Ati, J. Mater. Sci. Lett. 11 (1992) 581.
13. H. Rawson, Properties and Applications of Glasses, Elsevier,Amsterdam, 1980.
14. M.A.Chaudhry, A.M.Rana, M.Altaf, M.S.Bilal, Aust.J.Phys.48(1995)887.
15. J. Anjaiah ,C.Laxmikanth , N.Veeraiah , P.Kistaiah, Journal ofLuminescence,161(2015)147.
16. Liaolin Zhang, Guoping Dong, MingyingPeng, JianrongQiu, SpectrochimicaActa Part A, 93 (2012) 223.
17. CzeslawKoepke , MarcinSroda , AgnieszkaMarczewska , Krzysztof Wisniewski , PawełPichniarczyk, Journal of Luminescence ,179(2016)139.
18. Joanna Pisarska, WojciechA.Pisarski ,DominikDorosz , Jan Dorosz, Journal of Luminescence,171(2016)138.

C_02:Optical properties of Nd^{3+} doped BaF_2-ZnO-B_2O_3 Oxyflouride glasses

N.B. Shigihalli [1],Yogesh[1], Ashok Gowda[1], R. Rajaramakrishna[2]*

[1] Soundarya Institute of Management and Science, Soundarya Nagar, Sidedahalli, Bengaluru-73,
[2,] Department of Post-Graduate Studies & Research in Physics, The National College, Jayanagar, Bangalore – 560070, India*
Corresponding author r.rajaramakrishna@gmail.com

Abstract

Nd^{3+}-doped oxyflouride glasses of composition $20BaF_2$-$20ZnO$-$(60-x)B_2O_3$ - xNd_2O_3 (where x= 0, 1, 2, 3, 4 mol %) have been synthesized by melt-quenching technique. XRD and DSC results confirm glassy nature of the samples. Optical absorption studies reveal that the values of band gap decrease from 3.366 to 3.304eV with increase in Nd_2O_3 concentration. Judd-Ofelt (JO) analysis based on UV-Visible absorption spectra were performed to determine JO parameters Ω_λ (λ = 2, 4, and 6). The observed trend is $\Omega_6 > \Omega_2 > \Omega_4$ for all samples.All glass systems have $\frac{A_{em}}{A_{ESA}} > 1$ suggesting that in the prepared glasses amplification can occur. Radiative properties such as radiative transition probabilities, branching ratios and radiative lifetimes have been estimated. The lifetimes for the $^4F_{3/2}$ level are found to decrease with increases in Nd_2O_3 concentration. $^4F_{3/2} \rightarrow {}^4I_{11/2}$ transition has relatively higher branching ratio and has energy 9595 cm^{-1} which corresponds to wavelength 1.0422 µm. Radiative properties results show that these glasses could be potential laser materials.

PACS :78.66.Jg, 78.40.Pg, 78.40.Fy, 78.40.Ha

1. Introduction

Rare earth ions play an important role in modern technology as active ions in many optical devices because of abundant number of the absorption and emission bands arising from the transitions between the rare earth elements energy levels [1]. Incorporation of rare earth ions in different host materials modifies, significantly, the optical properties of the original material. The increasing importance of glasses doped with rare-earth ions as possible lasing materials has created considerable interest in the study of their optical properties. Nd^{3+} ion has been studied in a variety of glasses due to its potential application in the field of infrared laser and optical amplification [2]. For Nd^{3+} ion, the particular interest is correlated with the radiative transition $^4F_{3/2} \rightarrow {}^4I_{11/2}$, which presents laser transition at about 1.06 µm [3]. B_2O_3 is one of the best and well known glass former, which possesses high transparency, low melting point, high thermal stability, and good rare earth ions solubility. Zinc borate glasses have proved to be interesting hosts for lanthanide ions, both from a fundamental and an applied point of view [4]. Oxyflouride glasses doped with rare earth ions are one of the most attractive hosts because of their good physical and chemical properties like oxide glasses and excellent optical properties like fluoride glasses [5-7]. Among the fluorides, BaF_2 is an ideal host for rare earth ions since it has excellent solubility with

rare earth ions. Glass which possesses lower phonon energies has been proved to the most stable host for rare earth ions. BaF_2 possesses lower phonon energy 346 cm^{-1}[8, 9].

To understand the effect of rare earth ion Nd^{3+} on oxyflouride glass, we have undertaken the study of optical properties of oxyflouride zinc borate glasses of composition BaF_2 – ZnO - B_2O_3 (BZB) doped with different concentrations of Nd_2O_3.

2. Experimental

Neodymium oxide doped oxyflouride glasses were prepared by using appropriate amounts of BaF_2, ZnO, H_3BO_3 and Nd_2O_3 of high purity. The raw materials were thoroughly mixed in 12 gm batches. The mixture was then melted in a porcelain crucible at 950^0C by placing in a muffle furnace. The homogeneous melt was quickly quenched between two brass plates. Glass samples of about 2mm thickness were obtained. Powder XRD measurements were carried out by using Philips X'Pert pro multipurpose X-ray diffractometer (employing monochromatic Cu-Kαradiation). Differential thermal measurements were carried out using a Mettler Toledo Differential Scanning Calorimeter (DSC) in the temperature range 100^0C - 550^0C at a heating rate of 10^0C per min. Density of the bubble-free glass samples were measured by employing Archimedes principle using Tolueneas an immersion liquid. The refractive index of the samples was measured by using Abbe refractometer by using a sodium vapor lamp at wavelength of 589.3 nm. Room temperature UV- Visible absorbance spectra in the wavelength range 300- 1000 nm of polished samples were recorded using spectrophotometer.

3. Results and discussion

3.1 Physical properties

Average molecular weight of the multi-component glass system was calculated using the relation

$$M_{av} = X_{BaF_2}Z_{BaF_2} + X_{ZnO}Z_{ZnO} + X_{B_2O_3}Z_{B_2O_3} + X_{Nd_2O_3}Z_{Nd_2O_3} \quad (1)$$

Where X_{BaF_2}, X_{ZnO}, $X_{B_2O_3}$ and $X_{Nd_2O_3}$ are the mole fractions of the constituent oxides and Z_{BaF_2}, Z_{ZnO}, $Z_{B_2O_3}$ and $Z_{Nd_2O_3}$ are the molecular weights of the constituent oxides.

Molar volume (V_M) was calculated using the relation

$$V_M = \frac{M_{av}}{\rho} \quad (2)$$

The number density N of the Nd^{3+} ions was calculated using the relation [10]

$$N = \frac{x\,\rho N_A}{M_{av}} \quad (3)$$

Where x is the mole fraction of rare - earth oxide, ρ is the density of the glass, N_A is Avogadro's number and M_{av} average molecular weight of the glass.

Calculated values of the important physical properties are presented in Table 1. It can be observed that an increase in the Nd_2O_3 content influences the refractive index, density and also various other physical quantities. The density is found to increase with increase in Nd_2O_3 content. This is due to replacement of lower molecular weight oxide B_2O_3 with higher molecular weight of oxide ions Nd_2O_3 in the glass network.

Table 1. Important physical quantities of Nd^{3+} doped BZB glasses

.

Physical property	BZBN1	BZBN2	BZBN3	BZBN4
Density, ρ (g/cm^3)	4.753	4.824	4.905	4.948
Refractive Index, n at 589.3nm	1.625	1.632	1.641	1.652
Average molecular weight, M_{av} (g)	127.669	129.797	131.926	135.054
Molar Volume , V_M (cm^3/mol.)	26.860	26.906	26.895	27.294
Nd^{3+} -ion Concentration, N ($X10^{20}$ ions per cm^3)	2.242	4.476	6.718	8.826
Optical path length, t (cm)	0.189	0.201	0.196	0.194
Optical Band Gap, E_{opt} (eV)	3.366	3.327	3.325	3.304

3.2 XRD and DSC measurements

XRD profiles of undoped BZBN0 and doped BZBN1 glasses scanned at the rate of 2^0/min. for the 2θ values between 10^0 and 80^0 are shown in Figure 1. Absence of sharp peaks and broad hump around 27^0 indicate amorphous nature of the prepared samples.

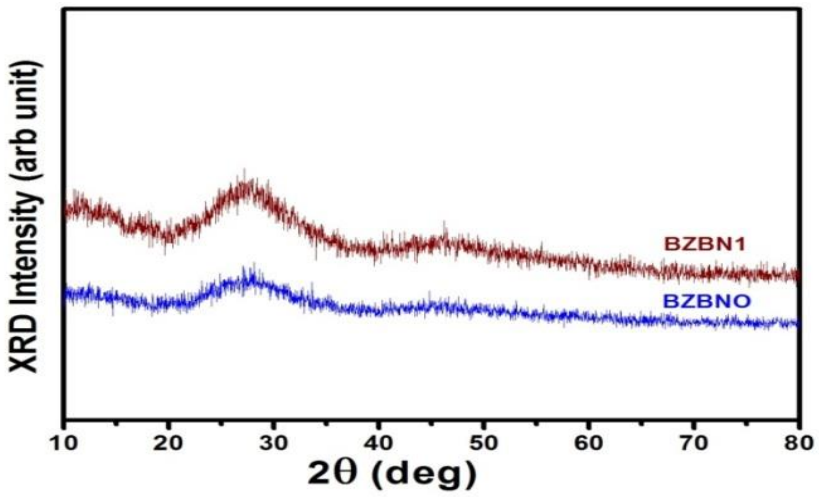

‘Fig.1. XRD profiles of undoped (BZBN0) and 1mol% (BZBN1) of Nd^{3+}doped BZB glasses

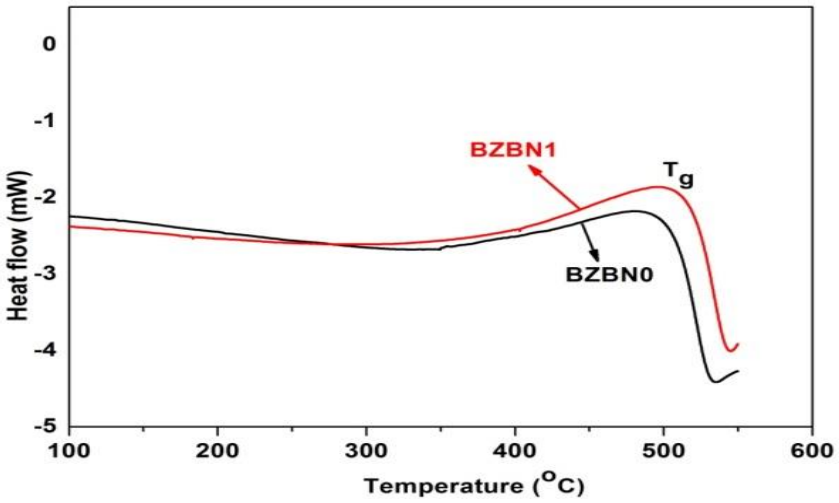

Fig. 2. DSC thermograms of undoped (BZBN0) and 1mol% (BZBN1) of Nd^{3+}doped BZB glasses

DSC thermograms of undoped BZBN0 and doped BZBN1 samples obtained in the temperature range 100^0C - 550^0C at a heating rate of 10^0C per min. are shown in Figure 2. It shows the existence of transition temperature (T_g) and there by confirming glassy nature of prepared samples. The value of glass transition temperature for undoped BZB glass is 488^OC and for 1 mol% Nd^{3+} doped BZB glass is 502^OC. Higher values of glass transition temperature shows that the prepared glass samples are covalent bonded.

4. Optical properties

4.1 Absorption spectra

The room temperature UV-Visible absorption spectra of Nd^{3+} doped BZB glass samples recorded is as shown in Figure 3. It has ten absorption bands with different relative intensities. These absorption bands are due to transitions from ground state $^4I_{9/2}$of Nd^{3+} to higher energy states inside the $4f^3$ electronic configuration of the Nd^{3+} ions. The absorption intensity increases with increase in concentration of Nd_2O_3. The absorption bands are relatively broad because of amorphous nature of samples and are not pure Gaussian.

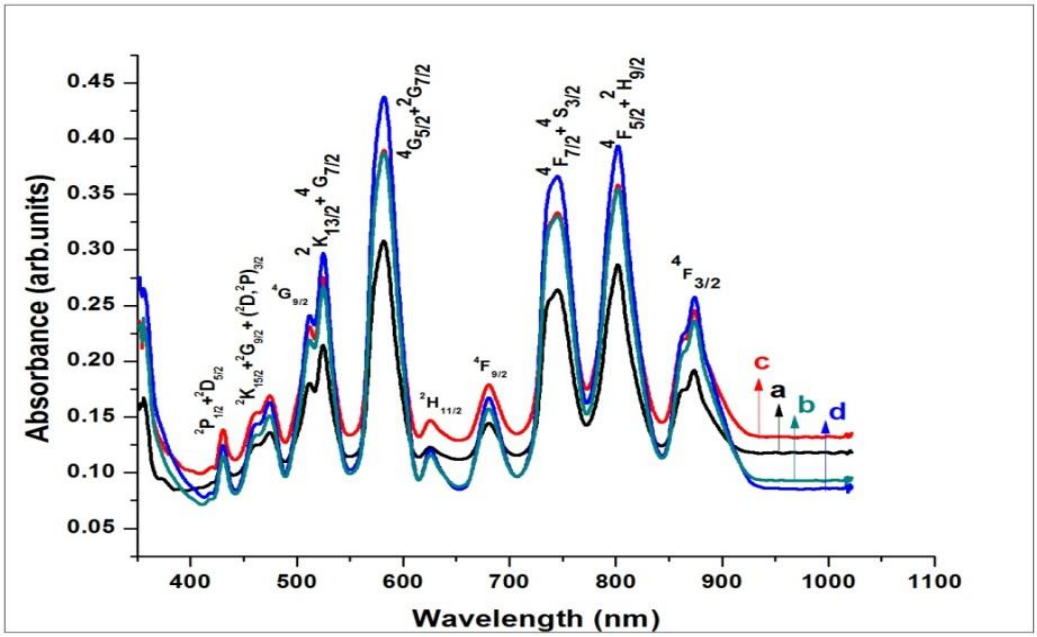

Fig. 3. UV-Visible absorption spectra of (a) 1 mol% (b) 2 mol% (c) 3 mol % and (d) 4 mol% of Nd^{3+} doped BZB glasses.

4.2 Optical band gap

The study of optical edge is useful for understanding the optically induced transitions and optical band gaps of materials. In order to study the optically induced transitions, optical band gaps have been computed from the UV-Visible absorption spectra of the glasses. The relation between absorption coefficient $\alpha(\nu)$ and the photon energy $h\nu$ of the incident radiation is given by the relation [11]

$$\alpha(\nu) = \frac{B}{h\nu}\left(h\nu - E_{opt}\right)^n \qquad (4)$$

This relation can be written as

$$(\alpha h\nu)^{\frac{1}{n}} = B\left(h\nu - E_{opt}\right) \qquad (5)$$

Where *B* is a constant called band tailing parameter, $h\nu$ is the photon energy and E_{opt} is the optical energy band gap. Values of *n* are 1/2 and 2 for direct and indirect forbidden transitions respectively [12].The absorption coefficients $\alpha(\nu)$ were determined near the absorption edge at different photon energies ($h\nu$) for all glass samples. It is well known that for amorphous materials a reasonable fit of equation (5) with n=2 is achieved [13].

The typical plot of $(\alpha h\nu)^{1/2}$ versus photon energy $h\nu$ (Tauc's plot) is as shown in Figure 4 for indirect allowed transitions.

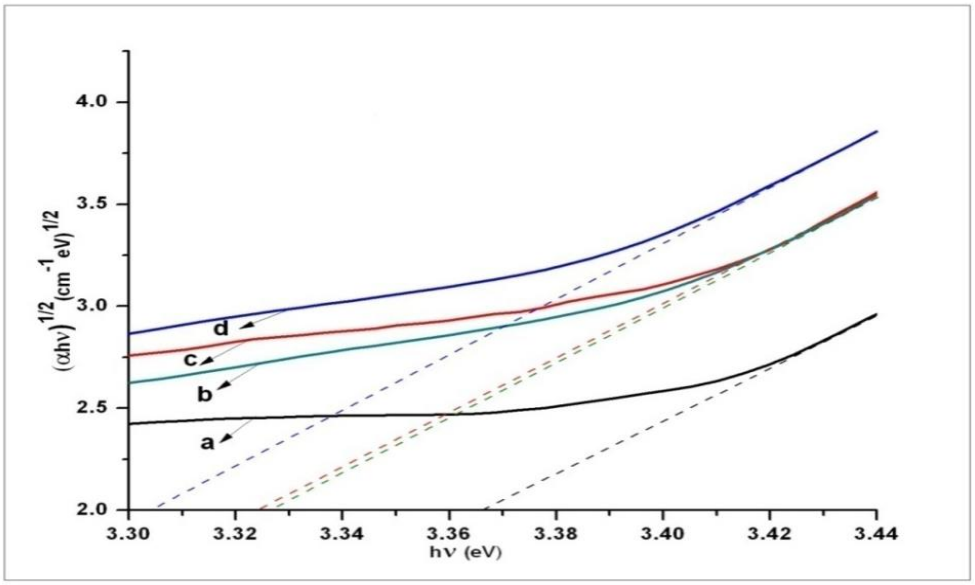

Fig. 4. Tauc's plot for (a) 1 mol% (b) 2 mol% (c) 3 mol % and (d) 4 mol% of Nd^{3+} doped BZB glasses.

The values of band gap (E_{opt}) are obtained by extrapolating the linear region of the curves to meet the hν axis at $(\alpha h\nu)^{1/2} = 0$. The values obtained are 3.366, 3.327, 3.325 and 3.304 eV for BZBN1, BZBN2, BZBN3 and BZBN4 glasses respectively. It can be observed that the optical band gap slightly decreases with the increase of Nd_2O_3 concentration which is likely due to the increase of bonding defect and non-bridging oxygen.This leads to an increase in the degree of electrons localization and there by the increase of donor center in the glass matrix. The increase of presence of donor centre leads to the decreases of optical band gap, therefore, the shift of absorption edge toward the longer wavelength was observed [13].

4.3 Judd-Ofelt analysis

The absorption spectra (Figure 3) of Nd^{3+} doped BZB serve as a basis for evaluating radiative properties. The Judd-Ofelt (JO) theory [14, 15] has been used to investigate radiative nature of trivalent rare earth ions in a variety of laser host materials [16]. The intensity parameter, radiative life time and branching ratio are calculated with refractive index using JO analysis. The experimental oscillator strength (f_{exp}) was calculated from the absorption spectra by using the equation

$$f_{exp.} = 4.32 \times 10^{-9} \int \varepsilon(\nu) d\nu \qquad (6)$$

where $\varepsilon(\nu)$ is the molar absorptivity of a band at mean energy ν (cm^{-1}). $\int \varepsilon(\nu)\, d\nu$ is evaluated by measuring the area under the curve.

According tothe JO theory, the calculated oscillator strength for an induced electric-dipole and magnetic dipole transition from the ground state ΨJ (assumed that all the crystal-field split levels of the ground state are equally populated) to an excited state $\Psi' J'$ *is* given by

$$f_{cal} = \frac{8\pi^2 mc\nu}{3h(2J+1)}\left[\frac{(n^2+2)^2}{9n} S_{ed} + nS_{md}\right] \qquad (7)$$

In this equation, m is the mass of the electron, c is the speed of light, ν is the mean energy of the transition, '*J* ' is the total angular momentum of the ground state, h is the Planck's constant, (2J + 1) is the degeneracy of the ground state of the Nd^{3+} ion, n is the refractive index of the medium, $(n^2+2)^2/9n$ is the Lorentz local field correction and accounts for dipole-dipole correction, S_{ed} is the electric dipole line strength and S_{md} is the magnetic dipole strength. S_{md} can be neglected in comparison to S_{ed} , since in the case of Nd^{3+} ion, the bands produced by the magnetic dipole mechanism have very low spectral intensity compared to that of the electric dipole bands [17] S_{ed} is given by

$$S_{ed} = e^2 \sum_{\lambda=2,4,6} \Omega_\lambda (\Psi J \| U^\lambda \| \Psi' J')^2 \qquad (8)$$

Ω_λ (λ = 2, 4, 6) are JO intensity parameters, $\|U^{(\lambda)}\|^2$ are the doubly reduced matrix elements evaluated in the intermediate coupling approximation for a transition $\Psi J \rightarrow \Psi' J'$. The reduced matrix elements $\|U^{(\lambda)}\|^2$ are found to be almost invariant to the environment therefore, we have used the values given by Carnall et al. for Nd^{3+} in aqueous solution [18]. Because of overlapping of the bands ($^4F_{5/2}$ +$^2H_{9/2}$, $^4F_{7/2}$+$^4S_{3/2}$, $^4G_{5/2}$ + $^2G_{7/2}$, $^2K_{13/2}$ +$^4G_{7/2}$, $^2K_{15/2}$+ $^2G_{9/2}$+ (^2D, $^2P)_{3/2}$, $^2P_{1/2}$+ $^2D_{5/2}$) some are treated as single band with an appropriate combination of the respective reduced matrix elements. The values of reduced matrix elements, the mean wavelength and energy of the chosen absorption bands of Nd^{3+} doped BZB glasses are presented in Table 2.

Table 2. Values of reduced matrix elements for the chosen absorption bands of Nd^{3+} doped BZB glasses.

Transition from ground state $^4I_{9/2}$ →	Wavelength nm	Energy cm^{-1}	$\|U^{(2)}\|^2$	$\|U^{(4)}\|^2$	$\|U^{(6)}\|^2$
$^4F_{3/2}$	874	11441	0.0000	0.2293	0.0549
$^4F_{5/2}$ +$^2H_{9/2}$	802	12468	0.0102	0.2451	0.5124
$^4F_{7/2}$+$^4S_{3/2}$	746	13404	0.0010	0.0449	0.6597
$^4F_{9/2}$	681	14684	0.0009	0.0092	0.0410
$^2H_{11/2}$	624	16025	0.0001	0.0027	0.0104
$^4G_{5/2}$ + $^2G_{7/2}$	582	17182	0.9736	0.5949	0.0673
$^2K_{13/2}$ +$^4G_{7/2}$	525	19047	0.0618	0.1572	0.0865
$^4G_{9/2}$	513	19493	0.0046	0.0608	0.0406
$^2K_{15/2}$+ $^2G_{9/2}$+ (^2D, $^2P)_{3/2}$	474	21097	0.0010	0.0388	0.0284
$^2P_{1/2}$+ $^2D_{5/2}$	428	23364	0.0000	0.0369	0.0021

The experimental oscillator strengths $f_{exp.}$ were used to obtain values of the JO intensity parameters Ω_λ (λ = 2, 4, 6) following the least square fitting method. The validity of the fitting is examined by comparing the experimental and theoretical oscillator strengths. The experimental and calculated oscillator strengths for an induced electric-dipole in the Nd^{3+} doped BZB glasses

along with their rms deviations are presented in Table 3. The calculated oscillator strengths from the JO theory agree quite well with the experimental oscillator strengths.

The quality of fit is estimated by δ_{rms} value using the relation [17]

$$\delta_{rms} = \left[\frac{f_{cal} - f_{exp}}{q-p}\right]^{1/2} \quad (9)$$

where q is the number of transitions and p is the number of parameters.

Table 3. Values of ($f_{expt.}$ x10^{-6}), ($f_{cal.}$ x10^{-6}) and rms deviations of Nd^{3+} doped BZB glasses.

Transition from ground state $^4I_{9/2}$ →	Energy cm^{-1}	BZBN1 f_{exp} f_{cal}		BZBN2 f_{exp} f_{cal}		BZBN3 f_{exp} f_{cal}		BZBN4 f_{exp} f_{cal}	
$^4F_{3/2}$	11441	1.404	1.355	1.170	1.685	1.375	1.919	1.497	2.086
$^4F_{5/2}$ + $^2H_{9/2}$	12468	5.033	4.593	5.560	5.340	6.431	6.269	6.780	6.739
$^4F_{7/2}$+$^4S_{3/2}$	13404	4.379	4.872	5.220	5.495	6.383	6.555	6.903	7.006
$^4F_{9/2}$	14684	0.275	0.375	0.794	0.429	0.358	0.508	0.521	0.545
$^2H_{11/2}$	16025	1.136	0.104	0.260	0.119	0.112	0.141	0.166	0.151
$^4G_{5/2}$ + $^2G_{7/2}$	17182	12.667	12.586	15.070	15.112	16.150	16.189	18.040	18.094
$^2K_{13/2}$ +$^4G_{7/2}$	19047	0.381	1.207	3.230	2.689	3.623	3.011	4.217	3.298
$^4G_{9/2}$	19493	1.761	0.907	2.680	1.535	2.692	1.257	2.864	1.361
$^2K_{15/2}$ + $^2G_{9/2}$ + (^2D, ^2P)$_{3/2}$	21097	0.870	0.788	1.180	0.945	1.281	0.916	1.686	0.991
$^2P_{1/2}$+ $^2D_{5/2}$	23364	0.194	0.357	0.280	0.486	0.298	0.547	0.352	0.597
rms deviation		0.878		0.474		0.548		0.633	

It can be noted from the Table 3 that δ_{rms} values are 0.878, 0.474, 0.548 and 0.633 for BZBN1, BZBN2, BZBN3 and BZBN4 glasses respectively. The small rms deviations obtained indicate a good fit between the experimental and calculated oscillator strengths confirming the validity ofJO theory.

4.4Judd-Ofelt parameters

The JO intensity parameters Ω_λ exhibit the influence of the host materials on the transition probabilities. The relative magnitudes of Ω_λ are useful to explain the bonding, symmetry and stiffness of the host matrices. Jorgenson and Reisfield [19] in their work noted that the Ω_2 parameter is indicative of the amount of co-valent bonding while the parameters Ω_4 and Ω_6 are related to the rigidity of the host matrix.

Table 4. JO and spectroscopic quality parameters for Nd^{3+} doped BZB glasses

JO and spectroscopic quality parameters	BZBN1	BZBN2	BZBN3	BZBN4
$\Omega_2 x10^{-20}$ cm^2	2.995	3.470	3.563	4.016
$\Omega_4 x10^{-20}$ cm^2	2.432	3.108	3.463	3.750
$\Omega_6 x10^{-20}$ cm^2	3.279	3.653	4.342	4.594
$\chi = \Omega_4 / \Omega_6$	0.741	0.850	0.797	0.816
A_{em} / A_{ESA}	1.426	1.328	1.494	1.423

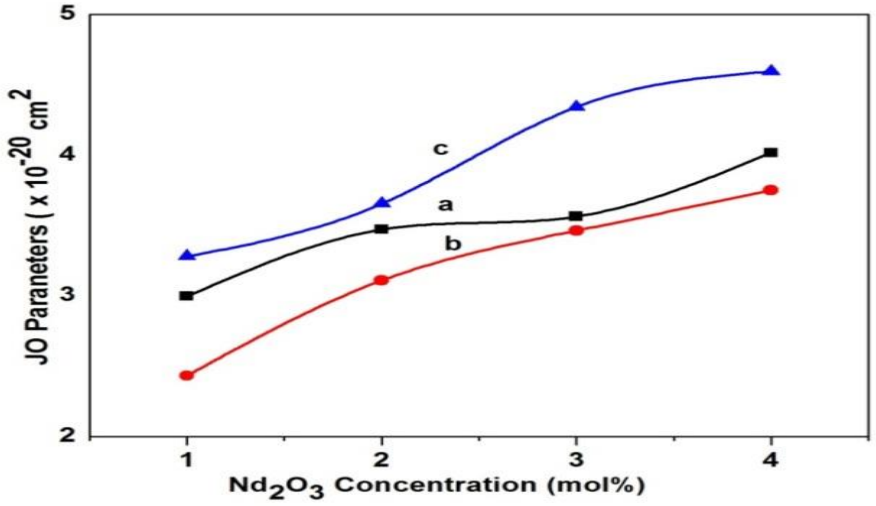

Fig. 5. Variation of JO parameters (a) Ω_2 (b) Ω_4 and (c) Ω_6 as a function of Nd_2O_3 concentration.

Ω_2, Ω_4 and Ω_6 were estimated using the squared reduced matrix elements and applying least square fit method are presented in Table 4.The variation of JO parameters as a function of Nd_2O_3 concentration is shown figure 5. In the present glass system, the observed trend is $\Omega_6 > \Omega_2 > \Omega_4$ for all samples. The increase in Ω_2 in the glasses with increase in Nd_2O_3 concentration indicates the increase of covalency between Nd^{3+}ions and ligands anions of the glasses. Further, it can be observed that the glass containing 4 mol % Nd^{3+} (BZBN4) possess the highest Ω_2 value which indicates the highest covalent character. The increase in Ω_4 and Ω_6 indicates that rigidity of the host increases with increase in Nd_2O_3 concentration.

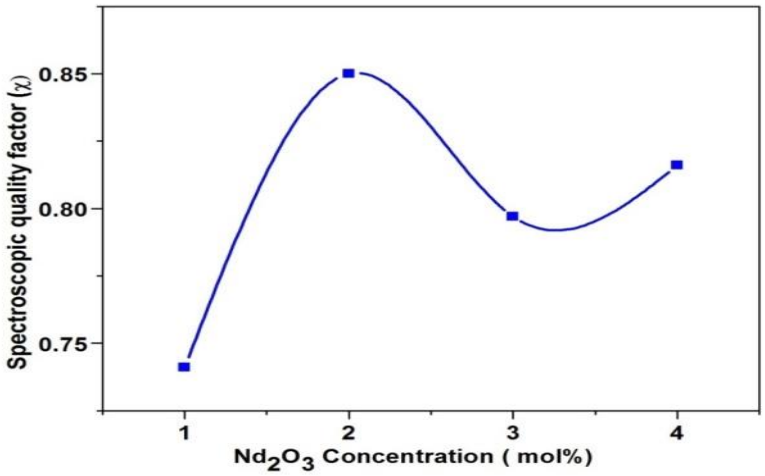

Fig. 6. Variation of spectroscopic quality factor (χ) as a function of Nd_2O_3 Concentration.

The emission intensity of the $^4F_{3/2} \rightarrow {}^4I_{11/2}$ transitions of Nd^{3+} could be characterized uniquely by the ratio of Ω_4 and Ω_6, called spectroscopic quality factor ($\chi = \Omega_4/ \Omega_6$) [20]. The calculated values of spectroscopic quality factor are presented in Table 4 and its variation as a function of Nd_2O_3 concentration is shown in Figure 6. The spectroscopic quality factor is related to odd crystalline fields and the relative intensities of the transition and determines the non-linear parameters of optical materials [21]. The smaller the value of χ , more intense is the $^4F_{3/2} \rightarrow {}^4I_{11/2}$ laser transition [22, 23]. The χ value for the BZBN1 glass system is 0.741 which is least compared to BZBN2, BZBN3 and BZBN4 glass systems. It shows that $^4F_{3/2} \rightarrow {}^4I_{11/2}$ is more intense laser transition in 1 mol% of Nd^{3+} doped BZB glass.

The JO parameters can also be used to estimate the emission (A_{em}) to Excited State Absorption (A_{ESA}) intensity ratio [24] is given by

$$\frac{A_{em}}{A_{ESA}} = \frac{0.21\,\Omega_6}{0.11\,\Omega_2 + 0.063\Omega_4} \qquad (10)$$

This ratio higher than 1 means the amplification can occur in the glasses [25]. In our work, all glass systems have $\frac{A_{em}}{A_{ESA}} > 1$ as presented in Table 4. This suggests that in the prepared glasses amplification can occur.

4.5 Hypersensitive transitions

The position and intensity of certain electric dipole transitions of rare earth ions are found to be very sensitive to the environment of the rare earth ion. In J-O theory those transitions in which intensity are dominated by the Ω_2 parameter were called hypersensitive transitions by Jorgenson and Judd [26]. For Nd^{3+} ion, $^4I_{9/2} \rightarrow {}^4G_{5/2} + {}^2G_{7/2}$ is the hypersensitive transition. It follows the selection rules $|\Delta J| \leq 2$, $|\Delta L| \leq 2$ and $\Delta S=0$. The values of $\left\|U^{(2)}\right\|^2$ for the hypersensitive transitions are much higher compared to other absorption levels of a particular rare earth ion. In the present work, the transition $^4I_{9/2} \rightarrow {}^4G_{5/2} + {}^2G_{7/2}$ which correspond to energy 17182 cm^{-1} has highest value 0.9736 (Table 2) of reduced matrix element $\left\|U^{(2)}\right\|^2$.

4.6 Radiative properties

The JO parameters along with refractive index (n) have been used to calculate the radiative transition probability, branching ratio and radiative lifetime of the excited state $^4F_{3/2.}$ The radiative transition probability (A_{rad}) for a transition $\Psi J \rightarrow \Psi' J'$ for an electric dipoleemission has been determined using the relation [27]

$$A_{rad}(\Psi J, \Psi' J') = \frac{n(n^2+2)^2}{9} S_{ed} \quad (11)$$

The total radiative emission probability ($A_T(\Psi J)$) of an excited state is the sum of the $A(\Psi J, \Psi' J')$ terms calculated over all the terminal states

$$A_T(\Psi J) = \sum A_{rad}\ (\Psi J, \Psi' J')$$

A_T is related to the radiative lifetime (τ_R)of an excited state by

$$\tau_R(\Psi J) = \frac{1}{A_T(\Psi J)} \quad (12)$$

The branching ratio (β_R) corresponding to the emission from an excited $\Psi' J'$ level to its lower level ΨJ is given by

$$\beta_R(\Psi J, \Psi' J') = \frac{A(\Psi J, \Psi' J')}{A_T(\Psi J)} \quad (13)$$

The JO parameters have been used to predict total radiative transition probability (A_{rad}), radiative lifetime (τ_R) and fluorescence branching ratio (β_R) for $^4F_{3/2} \rightarrow {}^4I_{15/2,}{}^4I_{13/2,}{}^4I_{11/2,}$ and $^4I_{9/2}$ transitions using equations (11), (12) and (13) respectively. The results are presented in Table 5.

Table 5. Values of radiation transition probability (A_{rad}), branching ratio (β_R) and radiative life time (τ_R) of Nd^{3+} doped BZB glasses.

Transitions from $^4F_{3/2} \rightarrow$	Energy cm^{-1}	BZBN1 $A_{rad}\ s^{-1}\ \beta_R$	BZBN2 $A_{rad} s^{-1}\ \beta_R$	BZBN3 $A_{rad} s^{-1}\ \beta_R$	BZBN4 $A_{rad} s^{-1}\ \beta_R$
$^4I_{15/2}$	5549.0	10.72 0.0052	12.12 0.0049	14.66 0.0051	15.86 0.0050
$^4I_{13/2}$	7613.0	215.22 0.1049	243.17 0.0991	294.31 0.1019	318.34 0.1009
$^4I_{11/2}$	9595.0	1042.47 0.5079	1213.60 0.4948	1447,73 0.5010	1573.94 0.4988
$^4I_{9/2}$	11454.0	784.2 0.3821	983.73 0.4011	1132.93 0.3921	1247.36 0.3953
Total $A_{rad}\ s^{-1}$		2052.62	2452.62	2889.64	3155.51
τ_R µs		487	407	346	316

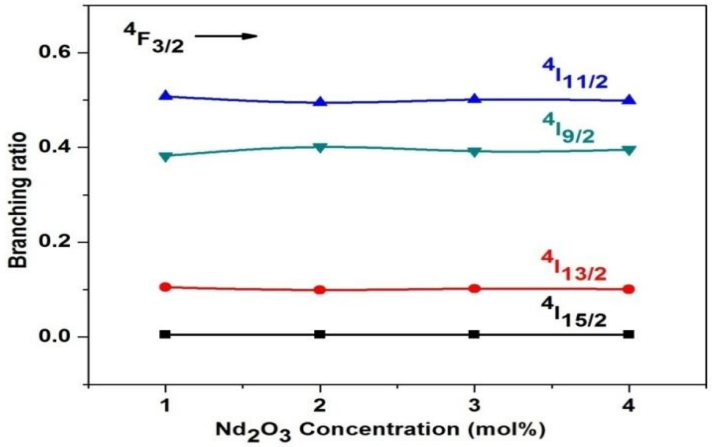

Fig. 7. Variation of branching ratio for $^4F_{3/2} \rightarrow {}^4I_{15/2}, {}^4I_{13/2}, {}^4I_{11/2}$, and $^4I_{9/2}$ transitions as a function of Nd_2O_3 concentration.

Variation of branching ratio for $^4F_{3/2} \rightarrow {}^4I_{15/2}, {}^4I_{13/2}, {}^4I_{11/2}$, and $^4I_{9/2}$ transitions concentration is shown in Figure in 7. It can be observed that the branching ratio is maximum for the $^4F_{3/2} \rightarrow {}^4I_{11/2}$transition and minimum for the $^4F_{3/2} \rightarrow {}^4I_{15/2}$transition in all glass compositions studied. The same result can also be observed in all Nd^{3+} doped glass hosts. Because of the high value of the transition probability for the $^4F_{3/2} \rightarrow {}^4I_{11/2}$transition, it can be expected that the stimulated emission cross-section is also a maximum for this transition.

In rare earth ions, Nd^{3+} ion has emerged as an excellent lasing ion at around wavelength 1.06 µm with a transition of $^4F_{3/2} \rightarrow {}^4I_{11/2}$ [28]. In our glass system, $^4F_{3/2} \rightarrow {}^4I_{11/2}$ transition has energy 9595 cm^{-1} which corresponds to wavelength 1.0422 µm.

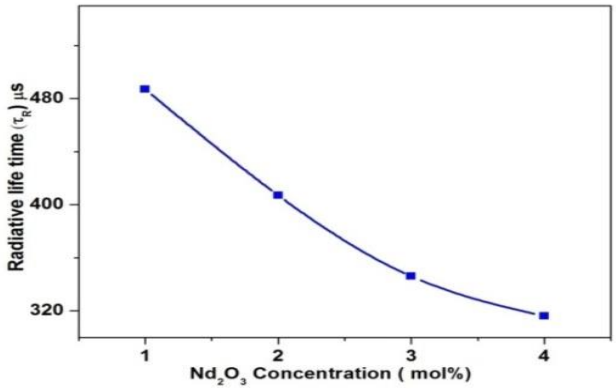

Fig. 8. Variation of radiative lifetime as a function of Nd_2O_3 concentration. The relatively higher branching ratio (Table 5) for $^4F_{3/2} \rightarrow {}^4I_{11/2}$ transition shows the suitability of the present glasses for laser applications. Variation of radiative life time as a function of Nd_2O_3 concentration is shown Figure 8. It can be observe that life time decrease with increase in Nd^{3+} ion concentration. This concentration dependent quenching of life time is attributed to the

increase in energy transfer process between Nd^{3+} ions through one of the cross-relaxation channels; $^4F_{3/2} + {}^4I_{9/2} \rightarrow {}^4I_{15/2} + {}^4I_{15/2}$ or $^4F_{3/2} + {}^4I_{9/2} \rightarrow {}^4I_{13/2} + {}^4I_{15/2}$ [29-31].

5. Conclusions

Optical properties of the glass samples of composition (in mol %) $20BaF_2$- 20ZnO - (60-x) B_2O_3 - xNd_2O_3 (x= 0, 1,2,3,4 mol %)were investigated. Optical band gap is found to decrease with increase in Nd_2O_3 concentration due to increase in non-bridging oxygen ions. JO parameters obtained from J-O theory follow the trend $\Omega_6 > \Omega_2 > \Omega_4$ for all the prepared glasses. The increase in Ω_2 in the glasses with increase in Nd_2O_3 concentration indicates the increase of covalency between Nd^{3+}ions and ligands anions of the glasses. The glasses have a small spectroscopic quality factor indicating that $^4F_{3/2} \rightarrow {}^4I_{11/2}$ laser emission is relatively intense. For all glasses, $\frac{A_{em}}{A_{ESA}} > 1$ suggest that the amplification can occur in all the prepared glasses. Decrease in life time with increase in Nd^{3+} ion concentration may be attributed due to the energy transfer through cross-relaxation between Nd^{3+} ions. $^4F_{3/2} \rightarrow {}^4I_{11/2}$ transition has the most potential for laser application with wavelength 1.0422 µm which corresponds to energy 9595 cm^{-1}. From the results of radiative properties it can be concluded that the prepared glasses could be potential laser materials.

Acknowledgements

One of the authors NBS wish to thank P B Kore, Chairman, K.L.E. Society, Belgaum and S C Hegadi, Principal, S Nijalingappa College, Bangalore for their continual encouragement to pursue higher studies.

References

1. M.A.K. Elfayoumi, M.Farouk, M.G. Brik, M.M.Elokr, *J. of Alloys and Compounds* 492 712-716 (2010), **DOI**:10.1016/j.jallcom.2009.12.024.
2. K. Upedra Kumar, P. Babu, Kyoung Hyuk Jang, Hyo Jin Seo, C.K Jayashankar, A.S. Joshi, *J. of Alloys and Compounds* 458 508-516 (2008),INIST-CNRS, Cote INIST : **1151**, **35400019593665.0900.**
3. Marcelo C. Silva, F.H. Cristovan, C.M. Nascimento, M.J.V.Bell, W.O. Cruz, A. Marletta *J. Non-Cryst Solids* 352 5296-5300 (2006),**DOI**:10.1016/j.jnoncrysol.2006.08.023
4. Adolfo Speghini. Massinmo Peruffo, Maurizio Casarin, David Ajo, Marco Bettinnelli, *J. of Alloys and Compounds* 300 174-179 (2000), PII: S0925-8388(99)00718-5
5. Y. Wang, J. Ohwaki, *Appl. Phy.Lett.* 63 3268 (1993), Appl. Phys. Lett. 63, 3268 (1993), **DOI**: org/10.1063/1.110170.
6. S. Tanabe, H. Hayashi, T. Hanada, N. Onodera, *Opt. Mater.* 19 343 (2009).
7. P.A.Tick, N.F. Borrelli. L.K. Cornelius, M.A. Newhouse, *J.Appl. Phys.* 78 6367 (1995), **DOI**:10.1063/1.360518.
8. Xvsheng Qiao Xiamping Fan and Minquan Wang, *Scripta Materialia* 55 211 (2006), **DOI**:10.5277/oa120213
9. P. Nachimuthu, R. Jagannathan, V.N.Kumar, D.N. Rao, *J. Non-Cryst. Solids*, 217 215-223 (1997).,DOI:10.1016/S0022-3093(97)00151-8.
10. A.S. Rao, Y.N. Ahammed, R.R.Reddy, T.V.R.Rao, *Optical Materials*, 10 245-252 (1998), DOI:10.1016/S0925-3467(97)00055-4.
11. P. G. Pavani, S. Suresh, V. C. Mouli, Optical Materials 34 215-220 (2011),

DOI:10.1016/j.optmat.2011.08.016.
12.L.M. Sharaf El-Deen, M.S. AI Salhi, M. M. Elkholy, *J. of Alloys and Compounds* 465 333-339 (2008), DOI:10.1016/j.jallcom.2007.10.104
13.P. Chimalawong , J. Kaewkho, P.Limsuwan , *J. Physics and Chemistry of Solids* 71 965-970 (2010), DOI: 10.1016/j.jpcs.2010.03.044

14. B.R. Judd, *Phys. Rev*. 127 750 (1962), DOI:10.1103/PhysRev.127.750.
15.G.S. Ofelt, *J. Chem. Phys.* 37 511 (1962), DOI.org/10.1063/1.1701366.
16.S. Bharadwaj, R. Shukla, S. Sanghi, A. Agarwal, Inder Pal, *Interntional J. of Modern Engineering Research* 2 3829-3824 Sept.- Oct. (2012).
17.L. Jyothi, V.Venkatramu, P. Babu, C.K. Jayashankar, M. Bettinelli, G. Mariotto, A. Speghini, *Optic. Mat.*, 33 928 (2011),DOI: org/10.1016/j.optmat.2010.11.015.
18.W.T. Carnall, P.R. Field, K. Rajnak, *J. Chem. Phys*., 49 4430 (1968), DOI: org/10.1063/1.1669893.
19. C. K. Jorgenson & R Resifeld , *J. Less Common Metals*, 93 107 (1983), DOI: 10.1080/00268976400100321.
20.R.R. Jacobs and M. J. Weber, *IEEE J. Quantum Electronics*, 12 102 (1976),DOI:10. 1109/JQE.1976.1069101.
21.Li Cheng-Ren, Li Shu-Feng, Dong Bin, Cheng Yu-Qi, Yin Hai-Tao, Yang Jing, Chen Yu *Chin.Phys.B* 20 017803 (2011), DOI:10.1088/1674-1056/20/1/017803
22.R.C.Powell, *Physics of Solid-State Laser Materials*, Springer, New York, USA, (1998).
23.M. Ajroud, M. Haouari, H. Ben Ouada, H. Maaref, A. Brenier and C. Garapon, *J. of Phys: Cond. Matter*, 12 3181 (2000), DOI:10.1088/0953-8984/12/13/324.
24.Ju H. Choi, Alfred Margaryan, Ashot Margaryan, Frank G. Shi, and Wytze Van Der Veer, *Advances in Opto Electronics*, 10 1155 (2007), DOI: org/10.1155/2007/39892.
25.Ahmad Marzuki, *J.Mathematica Dan Sains, Maret*, 12 1 (2007).
26.C.K.Jorgenson and B. R. Judd, *Mol Phy.*, 8 281 (1964), DOI:10.1080/00268976400100321
27. R. Cases, M.A. Chamarro, R. Alcala, V.D. Rodriguez, *J. Lumin*., 509 48 (1991).
28.K. Upendra Kumar, V. A. Prathyusha, P. Babu, C.K. Jayasankar, A.S.Joshi, A. Speghini, M. Bettinelli, *Spectrochemica Acta Part A*, 67 702 (2007), DOI:10.1016/j.saa.2006.08.027.
29.C. K. Jayashankar, R. Balakrishnaiah, V. Venkatramu, A.S.Joshi, A.Speghini, M Bettinelli, *J. Alloys and Compounds* 451 697-701 (2008).
30.H. Ebendoriff - Heidepriem, W. Seeber, D. Ehrt, *J. Non-Cryst Solids* 183 191 (1995).
31.E. Liegard, J. L. Doualan, R. Moncorge, M. Bettinelli, Appl. Phys. B 80 985 (2005).

C_03: Study on capacitive type humidity sensors

G. Vijaya Kumar

Department of physics, Maharani's Science College for women, Bangalore-560001, India.

Ph-+91 8553507652

E-Mail- kumar973@rediffmail.com

ABSTRACT

In the present work, Pristine Polyvinyl alcohol (PVA) film was prepared by a simple, low cost solution casting method. Using pristine PVA film of 1 cm by 1cm, Ag – PVA - Ag, Ag - PVA –CdSe and Au - PVA –CdSe sensors have been fabricated using thermal evaporation. The variations of the capacitance of obtained sensor with the relative humidity are measured. Ag-PVA-Ag sensor is active in the region 27.0 RH (%)-32.0 RH (%), Ag-PVA- CdSe sensor is active in the region 21.1 RH (%)-23.6 RH (%) and Au -PVA -CdSesensor is active in the region 29.8 RH (%)-32 RH (%).

KEYWORDS*:* polyvinyl alcohol, sensor, sensing mechanism.

1. INTRODUCTION

Humidity sensors have gained increasing applications in industrial processing and environmental control. For manufacturing highly sophisticated integrated circuits in semiconductor industry, humidity or moisture levels are constantly monitored in vapor processing. There are many domestic applications, such as intelligent control of the living environment in the building, cooking control for microwave ovens, and intelligent control of laundry etc. In automobile industry, humidity sensors are used in rare window defoggers and motor assembly lines. In medical industry humidity sensors are usedrespiratory equipment**,** sterilizers, incubators, pharmaceutical processing, and biological products. In agriculture humidity sensors are used for green-house-air conditioning, plantation protection, soil moisture monitoring, and cereal storage. Organic polymer-based sensors are grouped into resistive type and capacitive type [1-3]. Today, capacitive type RH sensors represent more than 75% of the available humidity sensors in the market [4].

2. EXPERIMENTAL

2.1 Preparation of Pristine PVA film

Pristine PVA films were prepared using a solution casting technique. A required quantity of PVA was dissolved in double distilled water and then heated gently, using a water bath to prevent thermal decomposition of polymer. The hot solution was stirred until the polymer is completely dissolved and forming a clear viscous solution. This is called PVA stock solution and is filtered to remove air bubbles trapped in the solution while stirring and kept aside for required duration to get proper viscosity. Known quantity of obtained solution was poured on to a leveled clean glass plate and left to dry at room temperature. After 48hrs, the films were peeled off from the glass plate and kept in vacuum decicator [5-9].

2.2 Preparation of Ag-PVA-Ag, Au/Ag-PVA-CdSe sensors.

Pure PVA film of 1 cm by 1cm is selected for the preparation sensors The Vacuum coating unit with water circulation is switched on. The Pure PVA film placed in the substrate holder in the chamber of the coating unit. Silver sample in the form of Pieces is taken in the spiral boat fixed between LT electrodes. When the pressure is 10^{-6} Torr the sample (silver) was evaporated by heating the material with a resistively heated spiral boat by passing suitable current, 6A through the L.T. The film was taken out from the chamber after one hour and water circulation was continued for about 30 minutes after the DC was switched off.

Next the other side of the PVA film (upside down) is kept in the substrate holder with the mask having the small holes of diameter 0.5mm. The above procedure is repeated to get the silver dots of diameter 0.5mm on PVA film. Thus one side of PVA is complete silver film and the other side is silver dots resulting in Ag-PVA-Ag sensor (device). This device is used for the characterization. The schematic diagram of the Ag-PVA-Ag sensor thus fabricated is shown in Fig.1. The similar procedure is repeated for the fabrication of Ag/Au -PVA-CdSe sensors.

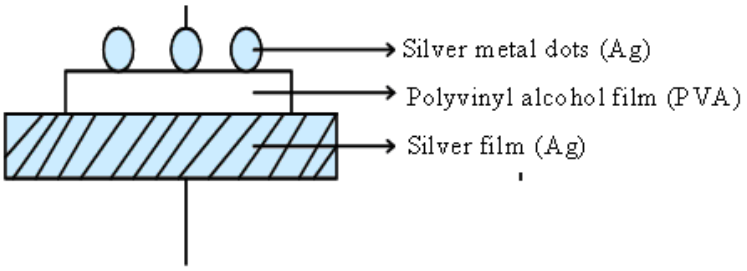

Fig.1. Ag-PVA-Ag sensor

2. RESULTS AND DISCUSSION

In capacitive type humidity sensor a common structure is either metal- insulator-metal (Ag-PVA-Ag) or metal- insulator- semiconductor (Au/Ag-PVA-CdSe). In this study polyvinyl alcohol (PVA) is used as an insulator.

Ag-PVA-Ag sensor is placed inside the humidity measurement chamber. The two ends of the leads of the sensor are connected to the LCR meter. The power is switched on the variation of the capacitance of Ag-PVA-Ag sensor with the relative humidity is measured. The same procedure is carried out for Au/Ag-PVA-CdSe sensors.

Ag-PVA-Ag sensor when the relative humidity is 27.0 (%), the capacitance is found to be 1.1 μF. As the relative humidity increases, water vapors penetrate into the porous of PVA causing an increase in the dielectric of the polymer and hence the capacitance changes to 5.9 μF at 32.0 RH (%). For further increase in relative humidity (%), the capacitance remains constant. This is mainly due to the presence of micropores in the insulator polymer PVA. Initially with increase in RH (%) water vapors penetrates the micropores resulting in an increase in capacitance. Once all the micropores completely filled with water then no more increase in the capacitance shown in figs. 2. The sensitivity of Ag-PVA-Ag and Au/Ag-PVA-CdSe sensors were better than the other reported sensors [10, 11, 12], however, the capacitance of Ag-PVA-Ag sensor was greater than the Au/Ag-PVA-CdSe sensors under the same conditions, possibly due to the type of electrodes used, since silver can create a better contact with the membrane surface than CdSe.

A similar behavior is observed even in Au/Ag-PVA-CdSe sensors with different active regions are plotted in fig.3 and fig.4

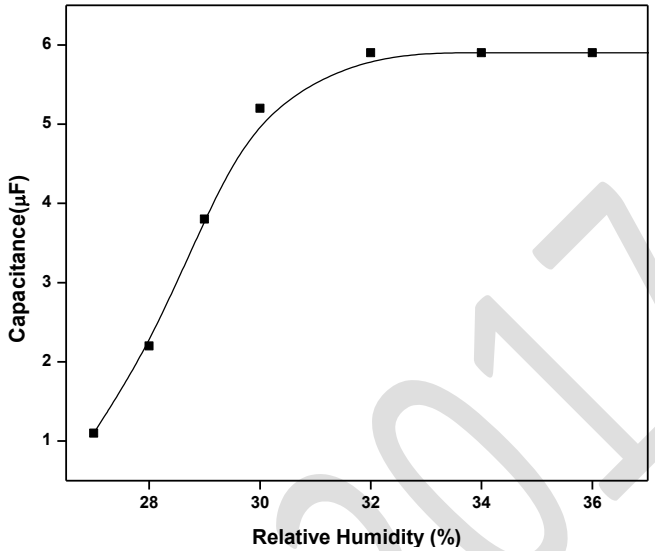

Fig.2. variation of capacitance with relative humidity of Ag-PVA-Ag sensor

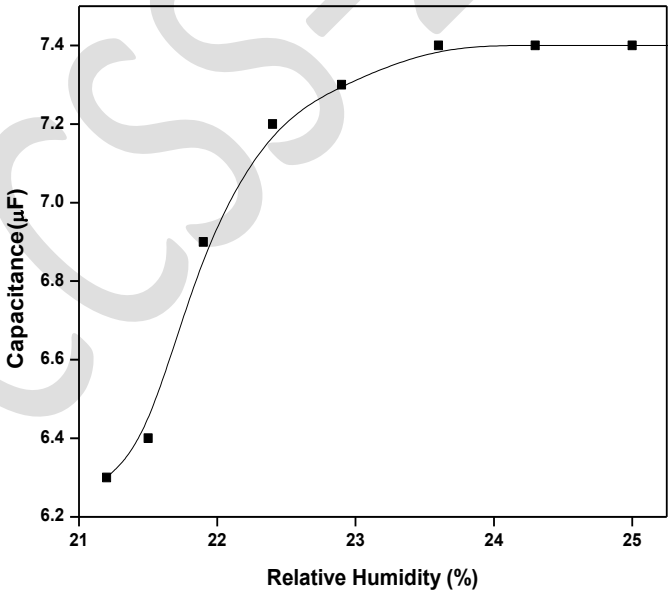

Fig.3. variation of capacitance with relative humidity of Ag-PVA-CdSe sensor

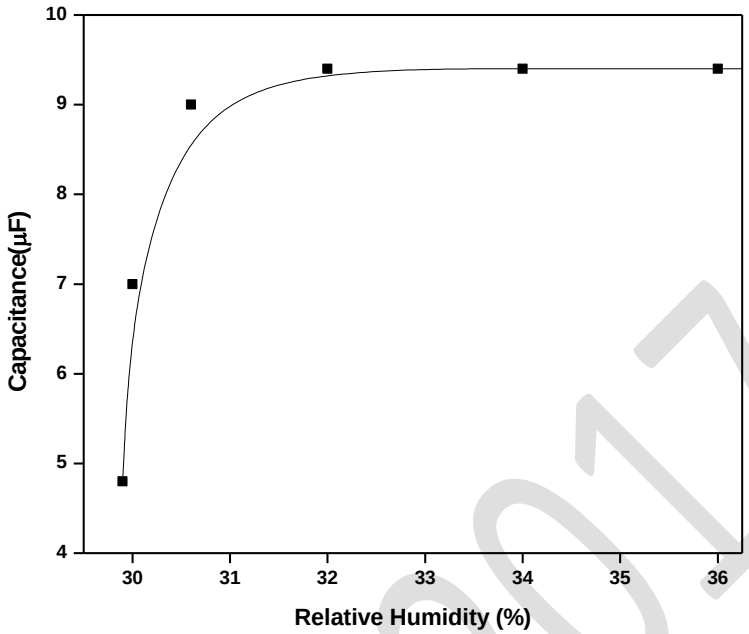

Fig.4. variation of capacitance with relative humidity of Au-PVA-CdSe sensor

3. CONCLUSION

In this paper, it was possible to apply a methodology to fabricate PVA film by a simple, low cost solution casting method and use, Ag – PVA - Ag, and Ag/Au - PVA – CdSesamples as capacitive humidity sensors. The sensing principle of the proposed sensors was based on the dielectric constant change of structures due to water vapor inside polymer PVA.

The variations of capacitance with RH (%) for Ag-PVA-Ag and Ag/Au -PVA-CdSe sensors have been studied and analyzed as follows.

Ag-PVA-Ag sensor is active in the region 27.0RH (%)-32.0RH (%) with the change in capacitance from 1.1μF- 5.9 μF, Ag-PVA-CdSe sensor is active in the region 21.1(%)-23.6RH (%) with the change in capacitance from 6.29μF- 7.40 μF and Au-PVA-CdSe sensor is active in the region 29.8(%)-32.0RH (%) with the change in capacitance from 4.7μF- 9.39 μF.

From the above investigations it reveals that there is noticeable change in capacitance with change in RH% mainly in the lower range ~32 RH (%). The measurements were reproducible and also Ag-PVA-Ag is potentially excellent sensing material for sensing low humidity because of their solubility in water.

REFERENCES

1. Packirisamy, M.; Stiharu, I.; Li, X.; Rinaldi, G. A Polyimide Based Resistive Humidity Sensor. Sens. Rev. **2005**, 25, 271–276.
2. Cho, N.-B.; Lim, T.-H.; Jeon, Y.-M.; Gong, M.-S. Inkjet Printing of Polymeric Resistance Humidity Sensor Using UV-Curable Electrolyte Inks. Macromol. Res. **2008**, 16, 149–154.
3. Matsuguchi, M. A Capacitive-Type Humidity Sensor Using Cross-Linked Poly(methyl Methacrylate) Thin Films. J. Electrochem. Soc. **1991**, 138, 1862.
4. Rittersma, Z.M. Recent Achievements in Miniaturised Humidity Sensors—A Review of Transduction Techniques. Sens. Actuators A Phys. 2002, 96, 196–210.
5. A. Tawansi, M.D. Migahed, and M.I. A. El-Hamid, Journal of polymer science: partB: polymer physics, **24 ,**2631-2642 (1986).
6. R.F Bhajantri et al, Polymer **47,** 3591-3598 (2006).
7. H.M. Zidan, Journal of applied polymer science, **88** ,104-111(2003).
8. R.I Mohamed, Journal of physics and chemistry of solids **61**, 1357-1361 (2000).
9. A. Tawansi et.al, Physica **B 254** 126-133 (1998).
10. Gu, L.; Huang, Q.A.; Qin, M. A novel capacitive-type humidity sensor using CMOS fabrication technology. *Sens. Actuators B Chem.* **2004**, *99*, 491–498.]
11. Chen, W.P.; Zhao, Z.G.; Liu, X.W.; Zhang, Z.X.; Suo, C.G. A Capacitive Humidity Sensor Based on Multi-Wall Carbon Nanotubes (MWCNTs). *Sensors* **2009**, *9*, 7431–7444.
12. Lee, H.; Lee, S.; Jung, S.; Lee, J. Nano-grass polyimide-based humidity sensors. *Sens. Actuators B Chem.* **2011**, *154*, 2–8.

C_04: Urban air electrical signatures at Jnanabharathi Campus, Bengaluru (12.96° N, 77.56° E)

Charan Kumar K[1], Sunil D Pawar[2], Murugavel P[2], Gopalkrishnan V[2], Kamsali Nagaraja[1*]

[1]*Department of Physics, Bangalore University, Bengaluru–560 056, INDIA*

[2]*Indian Institute of Tropical Meteorology, Pune-411008, INDIA*

email - dopcharan@gmail.com

Abstract

Simultaneous measurements of the atmospheric electrical conductivity (σ) and meteorological parameters were carried out at Jnanabharathi campus, Bangalore University (an urban station), Bengaluru, (12.96° N, 77.56° E) for the first time. Gerdien condenser setup for σ and mini boundary layer mast (micro meteorological tower) for weather parameters were used in this study. The observations show that the change in daily and weekly variations of σ is strong dependent of activity of Radon (^{222}Rn) gas and meteorological parameters (which defines the stability of the lower troposphere), respectively. The average σ for the study period was found to be 4.02 ± 0.02 x 10^{-14}S/m with higher values during winter compared to summer and monsoon. In future it is planned to use the air conductivity measurements for atmospheric stability, pollution and climate change studies

Keywords: atmospheric electrical conductivity, ionisation, small ions, radon

1 Introduction

The long-term variations in atmospheric electrical parameters are important for the studies of global electric circuit, thunderstorms and lightning activities. Emphasis in recent years in the field atmospheric electricity has shifted towards the precise understanding of the possible interaction of different sized aerosols with small air ions in atmospheric physics [1-4] and for geophysical applications[5-7]. Atmospheric electrical conductivity, electric field, air earth current (AEC) and small ion number density are important parameters for understanding the electrical nature of the atmosphere. The electrical conductivity of the air in an aerosol free atmosphere is mainly due to small ions. However, in a polluted atmosphere the small ions soon get attached to the aerosols to form the intermediate and large ions and contribute to air conductivity, which can alter the atmospheric electrical parameters[8,9]. Since, aerosols in air reduces the small ion concentration, the electrical conductivity have an inverse relationship with aerosol concentration and been often proposed to act as an index of aerosol loading in atmosphere [2, 10].

The conductive nature of air is due to these small ions in the lower troposphere which are determined mostly by radon (^{222}Rn), its progenies, gamma rays from soil and galactic cosmic radiations, in which contribution from gamma and cosmic radiations is almost constant near the surface. Hence, the variability of small ions near the surface is due to dynamics of activity of radon and its progenies[11]. ^{222}Rn is an inert and radioactive soil gas descending from uranium ^{238}U decay series with half-life 3.82 days. Radon is a gas 7.5 times heavier than air, when generated in Earth's crust; it penetrates the pores in the ground and moves upward by diffusion and convection toward the surface and into the air. This process is called exhalation and its rate depends on air pressure and also permeability, thermal gradient and humidity of the soil[12]. In the atmosphere, ^{222}Rn appears mostly in the vicinity of its source, i.e., ground, and its transport is determined by thermal processes.

The knowledge of atmospheric ions is important not only to understand the electrical state of the local atmosphere but also in understanding the global electric circuit[13-15]. It is necessary to fill the gaps in the data available, in respect of variation of atmospheric electrical parameters with orography over different locations in the lower troposphere[16]. Hence, for the first time, an attempt is made to analyze the data set of conductivity and associated meteorological parameters along with few radon gas measurements of fair weather days during January 2014 – December 2014, inside Jnanabharathi campus of Bangalore University, Bengaluru, India (12.59^0 N 77.57^0 E & altitude 920 m above mean sea level) and presented in this paper.

2. Experimental methodology

The Atmospheric Electricity Observatory and meteorological tower are located at the Jnanabharathi campus of Bangalore University (BU), Bengaluru, south India which is covered with moderate forest area.

2.1 Bipolar air conductivities and atmospheric radioactivity measurements

Atmospheric conductivity of both polarities was simultaneously measured using an aspirated Gerdien condenser tubes[17-19]. It consists of two identical cylindrical tubes of 10 cm diameter and 41 cm length joined by a U-shaped tube. The air was sucked in with a single fan and the shape of Gerdien condenser ensures that the flow of air is laminar, because turbulence flow can distort the accuracy of measurement. The inner co-axial electrode in both the tubes is of 1 cm diameter and 20 cm length. Opposite but equal potentials of ± 35 V are applied to the outer electrodes of the two condensers. The potential applied to the outer electrode will repel the same polarity ions towards the inner electrode generating an electrical pulse in both the pulses. The critical mobility of the instrument is greater than 10^{-4} $m^2V^{-1}S^{-1}$ and is capable of resolving the values of conductivity as small as 3×10^{-16} $\Omega^{-1}m^{-1}$ [(17)].

Zeroing of the system was performed by measuring the conductivity when fan and potential were switched off and are incorporated in the actual measurements[19].

Few atmospheric radon gas measurements were carried out using Genitron made Alpha GUARD PQ 2000 PRO[20] and it is a compact portable measuring system for the continuous monitoring of ambient gamma dose rate, radon concentration along with air temperature (T), relative humidity (RH) and pressure (P) with an inbuilt relocation sensor. Alpha guard is housed with a high resolution Geiger-Müller tube having measuring range of 20 nSv.hour-1 - 10 mSv.hour-1 with resolution of 1 nSv.hour-1 to measure ambient gamma dose. The ionization chamber in Alpha Guard is based on the principle of pulse ionization for measuring radon by 3D alpha spectroscopy technique with DSP technology with a range of 2–20,00,000 Bqm^{-3} and sensitivity of 4.5 CPM/100 Bqm^{-3}

2.2 Meteorological parameters

The department of Physics, Bangalore University, Bengaluru, India is equipped with two weather monitoring towers namely Mini Boundary Layer Mast and Automatic Weather Station under the network of Indian Space Research Organization, Government of India for micro-meteorological measurements to characterize the surface layer of atmosphere. Different atmospheric parameters like ambient temperature, relative humidity, air pressure, incoming and outgoing solar radiation, wind speed and wind direction, rain fall etc are continuously monitored at different heights Among all, only temperature and relative humidity data are used for the analysis. The parameters were measured at 1Hz sampling round the clock and was averaged for desired time intervals using a program. The quality control of data made by checking the validity of data and omitted erroneous values beyond 3-sigma values[21].

3. Results and Discussion

3.1 Nocturnal stability and mixing processes

The fair weather behaviour of nocturnal radon accumulation and air conductivity for continuous 4 days in January 2014 is shown in Figure 1. The higher value of activity of radon and air conductivity in early morning hours and subsequent decrease during afternoon hours immediately indicates conditions of high nocturnal stability, temperature inversions and good daytime mixing conditions, especially in the afternoon hours. This type of diurnal trend is well reported and frequently observed in the summer, rare in winter[22-24].

3.2 Diurnal variations

The diurnal variation of activity of radon along with the temperature and relative humidity for a typical fair weather day is shown in Figure 2. Activity of Radon varied between 2 – 66 Bq/m^3 with order of 33. The concentrations show maxima during the early morning hours,

generally between 0600 and 0830 h of Indian Standard Time (IST) and decreases after sunrise, attaining minima during the afternoon, 1400 to 1600 h of IST at BU [11, 24]. The in situ

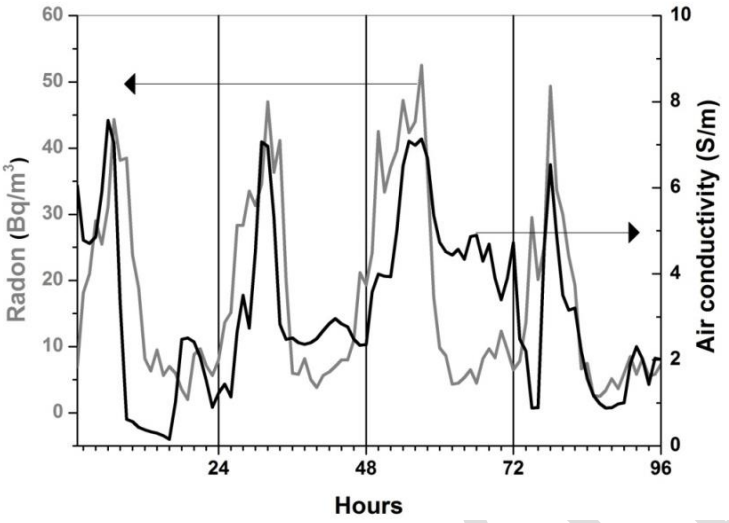

Figure 1: Nocturnal stability and mixing processes of radon and air conductivity

-diurnal cycle of radon is triggered by soil emission and atmospheric dynamics (primarily small-scale vertical mixing) and is well reported[25, 26].

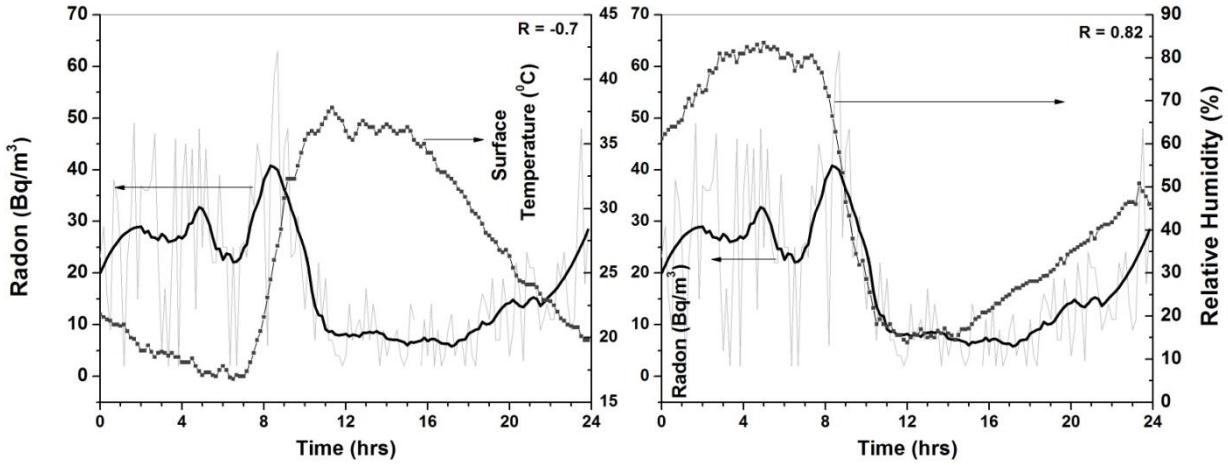

Figure 2: Diurnal variations of activity of radon

The diurnal variation of air conductivity (σ) along with temperature and relative humidity for a single fair weather day in the month January, April and August representing typical winter, summer and monsoon months, respectively are shown in Figures. 3&4.

The similar type of observations were obtained for most of fair weather days, thus, the observations described below can be reasonably generalized for other fair weather days as well. As reported earlier, an early morning peak and significant decrease during afternoon

hours was observed and there exists a negative correlation between σ & temperature and positive correlation between σ & relative humidity for the study period[23, 27]. And also it is

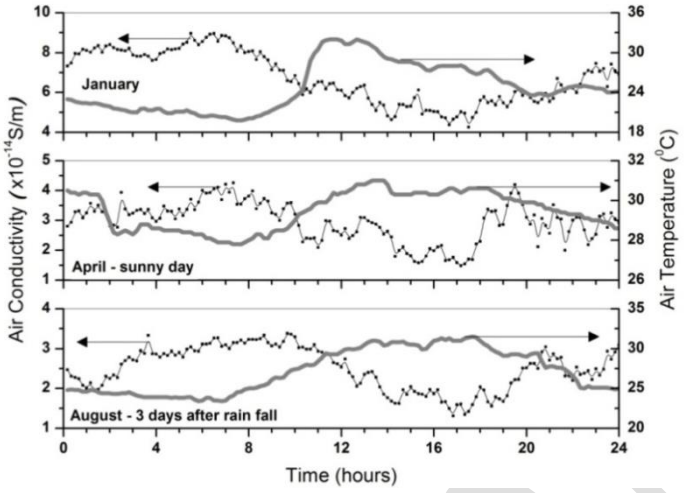

Figure 3: Diurnal variations of air conductivity with temperature for different months

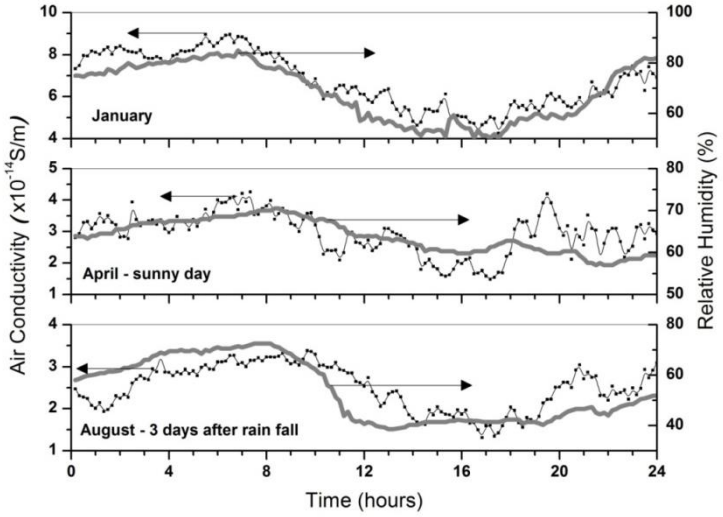

Figure 4: Diurnal variations of air conductivity with relative humidity for different months

found that the local radioactivity (radon and its progeny) plays very important role in defining the diurnal variation of air conductivity $(\sigma)^3$. The air conductivity, for given days (Figures 4 & 5), varied between 4.5 to 8.5 x 10^{-14}S/mfor January, 1.5 to 4.5 x 10^{-14} S/mfor April , 1.3 to 3.2 x 10^{-14} S/mfor August. In table 1, the experimentally measured values of air conductivity for different environments are compared with present observations.

Table 1: Comparison of air conductivity for different environments

Study Region (Elevation)	**Air Conductivity (X 10^{-15} S/m)**
Roorkee, India, (3 months) (268 m)	3.44 x 10^{-15} S/m [28]
Pune, India (560 m)	21.5 x 10^{-15} S/m [29]
Mysore, India (763 m)	34.8 x 10^{-15} S/m [23]
Maitri, Antarctica (103 m)	21 x 10^{-15} S/m [30]
Indian Ocean	2.9 - 7.8 x 10^{-15} S/m [31]
Arabian Sea	5 - 30 x 10^{-15} S/m [32]
Eskdalemuir, Scotland (245 m)	9.8 ± 0.7 x 10^{-15} S/m [33]
Berlin, Germany (34 m)	6 - 8 x 10^{-15} S/m [34]
Reading, UK (61 m)	3 - 9 x 10^{-15} S/m [34]
Immediately above the continental surface (Generally)	2 – 20 x 10^{-15} S/m & up to 40 x 10^{-15} S/min clean marine air [35]
Bengaluru, India (920 m)	40.2 ± 0.2 x 10^{-15} S/m [This Study]

From table 1, it is clear that experimentally observed air conductivity values are higher for higher altitude regions compare to lower altitude regions as theoretically estimated & reported[35]. But, the effect of pollution of air conductivity is not discussed in this section; as it needs sophisticated theoretical and experimental assessment for results which are planned in future.

The statistics of all the measured parameters is presented in table 2. As reported in south Indian region, the conductivity of air was higher during winter days compared to summer and monsoon. This may be due to possible occurrence of longer temperature inversions and trapping of radioactive gases near surface over Bengaluru and the measured air conductivity values are comparable with other results of similar environments.

2014	Air Conductivity (x 10^{-14} S/m) [±SE on mean]	Temperature (^{0}C)	RH (%)	No of days
Jan	**7.44 ± 0.03**	**22.06**	**55.52**	**21**
Feb	**6.14 ± 0.03**	**23.95**	**37.72**	**19**
Mar	**3.70 ± 0.02**	**26.10**	**43.13**	**18**
Apr	**3.90 ± 0.04**	**28.07**	**46.16**	**18**
May	**1.55 ± 0.01**	**27.04**	**60.60**	**9**
Jun	**2.19 ± 0.02**	**25.41**	**68.84**	**15**
Jul	**1.47 ± 0.02**	**23.51**	**75.14**	**11**
Aug	**0.93 ± 0.01**	**23.31**	**77.28**	**14**
Sep	**1.42 ± 0.01**	**23.94**	**72.70**	**14**
Oct	**4.80 ± 0.02**	**23.29**	**76.30**	**16**
Nov	**7.16 ± 0.01**	**22.18**	**65.98**	**21**
Dec	**7.54 ± 0.03**	**21.85**	**66.35**	**17**
Average	**4.02 ± 0.02**	**24.22**	**62.14**	**16**

Table 2: Complete statistics of air conductivity along with selected meteorological parameters

Conclusion

The measurements of bipolar air conductivities and meteorological parameters are carried out during January – December, 2014 at Jnanabharathi Campus, Bangalore University, Bengaluru (12.96° N, 77.56° E), India for the first time. The study was carried out, in order to see the urban electrical signatures of atmospheric air for Bengaluru environment and relate them with meteorological parameters. The observed values of air conductivity are comparable with the earlier results in similar environments of India. A well defined diurnal variation in conductivity suggests its dependence on several meteorological parameters. We observed a significant effect of atmospheric convective instability on the air conductivity also. The average air conductivity for the study period was found to be 4.02 ± 0.02 x 10^{-14}S/m with higher values during winter compared to summer and monsoon. In future it is planned for simultaneous measurements with local radioactivity and to use the same for atmospheric stability, pollution and climate change studies.

Acknowledgements

Authors are thankful to the Director, National Atmospheric Research Laboratory for the constant encouragement and extending all the facility to carry out the experiments at Gadanki and Indian Space Research Organization (ISRO), Government of India for financial assistance to carry out the present research work**.**

References

1. Misaki M & Takeuti T, *J Meteor Soc. Japan*, 48 (1970) 263
2. Kamra A K & Deshpande C G, *J Geophys Res*, 100 (1995) 7105
3. Nagaraja Kamsali, Prasad B S N & Jayati Datta, *Adv Space Res*,44 (2009) 1067
4. Jaan Salm & Eduard Tamm, *Aerosol Air Qual Res*, 11 (2011) 211
5. Liperovsky V A, Meister C V, Liperovskay E V & Bogdanov V V, *Nat Hazards Earth Syst Sci*, 8 (2008) 199
6. Pulinets S A, *Adv Space Res*, 44 (2009) 767
7. Mizuno A & Takashima K, *J Electrostat*, 71 (2013) 529
8. William A Hoppel & Glendon M Frick, *Aerosol Sci Technol*, 5 (1986) 1
9. Savita Dhanorkar & Kamra A K, , *J Geophys Res*, 98 (1993) 14895
10. Retalis D, Pitta A & Psallidas P, *Meteorol Atmos Phys*, 46 (1991) 197
11. Nagaraja K, Prasad B S N, Madhava M S, Chandrashekara M S, Paramesh L, Sannappa J, Pawar S D, Murugavel P & Kamra A K, *Radiat Meas*, 36 (2003) 413
12. Keller G & Schutz M, *Radiat Prot Dosim*, 24 (1988) 43
13. Roble Raymond G & Israel Tzur, *The Earth's Electrical Environment* (The National Academies Press, Washington) (1986) 206
14. Rycrofta M J, Israilsson S & Price C, *J Atmo Sol Ters Phy*, 62 (2000) 1563
15. Devendraa Siingh, Vimlesh Pant & Kamra A K, *J Geophys Res*, 112 (2007) doi: 10.1029/2006JD008101
16. Harrison R G & Carslaw K S, *Rev. Geophys*, 41 (2003) 1
17. Dhanorkar S S, Deshpande C G & Kamra A K, *Atmos Environ*, 23 (1989) 839
18. Karen Louise Aplin, *Instrumentation for atmospheric ion measurements*, Ph.D thesis, The University of Reading, Reading, United Kingdom, 2000
19. Kolarz P M, Filipovic D M, Marinkovic B P, *App Rad Isotopes*, 67 (2009) 2062
20. Chambers S D, Williams A G, Crawford J & Griffiths A D, *Atmos Che Phy, 15 (2015)* 1175-1190

21. Rao K G, Muhsi M, Reddy N N, Rao T N, Kumar M, Ananth A G, ... & Ramgopal K *PROWNAM. Scientific Report. ISRO-SR*, *2*. (2012)
22. Sesana L, Caprioli E, & Marcazzan G M, *J Envi Rad, 65* (2003) 147
23. Rani K P, Paramesh L & Chandrashekara M S, *J Envi Rad*, *138* (2014) 438
24. Prasad B S N, Nagaraja K, Chandrashekara M S, Paramesh L, & Madhava M S, *Atmos Res*, *76* (2005) 65
25. Wilkening M, *Radon in the Environment* (Elsevier Science Publishers, The Netherlands) (1990) 40
26. Porstendorfer J, *J Aero Sci, 25 (1994)* 219
27. Kumar V S, Sampath S, Das S M, & Kumar K V, *Geo J Inter, 122* (1995) 89.
28. Kumar A, *Ind J Phy, 87* (2013) 411
29. Nagaraja K, Prasad B S N, Srinivas N & Madhava M S, *J Atmos Solar Terr Phy, 68 (2006)* 757
30. Deshpande C G & Kamra A K, *J Geo Res: Atmos, 106 (2001)* 14207
31. Pawar S D, Murugavel P & Lal D M, *J Geo Res: Atmos*, *114* (2009) 2
32. Pawar S D, Siingh D, Gopalakrishnan V, & Kamra A K, *J Geo Res:Atmos, 110 (2005)* 10
33. Harrison R G & Bennett A J, *J Atmos Solar Terr Phy, 69 (2007)* 515
34. Bennett A, *Measurement of atmospheric electricity during different meteorological conditions*, PhD Thesis, University of Reading, Reading, 2007
35. Rycroft M J, Harrison R G, Nicoll K A & Mareev E A, *Space Sci Rev, 137 (2008)* 83

C_05: Quasi one-dimensional ZnO nanostructures for efficient detection of Hydrazine

Wajeeha Sultana[*a] *and B. Eraiah*[b]

[a]*Smt.V.H.D.C.I of Home science (Maharani's Science College for Women), Bangalore, India,*

[b]*Department of Physics, Bangalore University, Bangalore, India*

**Email id:wajeeha.sultana@gmail.com*

ABSTRACT

Nanosize ZnO prepared earlier using amines of different chain lengths, like hexyl amine (ZnO-H), octylamine (ZnO-O) and dodecyl amine (ZnO-D) as reactant were used to modify gold electrode for the detection of hydrazine. Electrocatalytic oxidation of hydrazine was investigated for a particular concentration (33 µM) of hydrazine by cyclic voltametry. Among the three electrodes prepared, ZnO-O, showed a best electrochemical current response for 33 µM concentration of hydrazine. This electrode was selected for further electrochemical studies. A detection limit of 3 nM is obtained with a signal to noise ratio of 5. Linearity range from 3 nM to 322 µM with a sensitivity of 1.5 µA μM^{-1} cm^{-2} is obtained.

KEY WORDS: Hydrazine, quasi one dimension, detection, zinc oxide, sensor

1. INTRODUCTION

Among the chemicals used in industry and laboratories, the compound hydrazine comes under high risk to human health. According to National Fire Protection Association, USA (NFPA) it carries a very high risk factor tag in terms of health and flammability and reactivity. Hydrazine is a highly reactive base and a powerful reducing agent. It is a suspected carcinogen. The chances of contamination of water bodies are high. Therefore to protect the environment and thus ensure the safety of human and marine health, it is very important to detect it in water samples. A large number of attempts have been made to detect hydrazine since many years using zinc oxide [1-5].

ZnO (II-IV), a semiconductor offers itself as a good electro catalyst because of its unique properties such as large band gap of 3.37 eV and high exciton binding energy of 60 meV. One-dimensional ZnO nanostructures are of particular interest because of its larger surface area and faster electron transfer.

More recently Rafiq Ahmad et al. have fabricated a hydrazine sensor using vertically-aligned Au/Zn**O** nanorods grown on electrode [6].A selective amperometric hydrazine sensor based on mesoporous Au/ZnO nanocomposites is prepared by Adel A. Ismail et al[7].Jie Hu et al have reported controllable synthesis of branched hierarchical ZnO nanorod arrays for highly sensitivehydrazine detection [8] and S.K. Mehta et alhave fabricated Ultra-high sensitive hydrazine chemical sensor based on low-temperature grownZnO nanoparticles [9]. In this report, we have used quasi one dimensional ZnO to fabricate an electrode for the detection of hydrazine. Synthesis and characterization of quasi one dimensional nanostructures of ZnO by using amines of different chain lengths, like hexyl amine (ZnO-H), octylamine (ZnO-O) and dodecyl amine (ZnO-D) as reactant has been reported in our earlier work [10]. The compounds were well characterized using powder XRD, UV-visible spectroscopy, IR spectroscopy, Scanning Electron Microscopy and Transmission Electron Microcopy.ZnO-H, ZnO-O and ZnO-D prepared are used to modify gold electrode for the detection of hydrazine. Among the three electrodes prepared, ZnO-O, showed a better electrochemical current response for 33 µM concentration of hydrazine. This is selected for further electrochemical studies. The response using only bare gold, that is without coating is many folds less [11]. A detection limit of 3 nM is obtained with a signal to noise ratio of 5. Linearity range from 3 nM to 322 µM with a sensitivity of 1.5 µA μM^{-1} cm^{-2} is obtained.

2.MATERIALS AND METHODS

2.1 Electrode fabrication

Polished gold electrodes were coated with ZnO-H, or ZnO-O or ZnO-D prepared. Using cyclic voltammetry, the electrodes were tested for 33 µM concentration of hydrazine in 0.2 M phosphate buffer solution. ZnO-O/Au showed maximum current response (3.3 µA) and that of ZnO-H stands in between these two with respect to both current and over potential. Considering this, ZnO-O/Au is chosen for further studies.

3 RESULTS AND DISCUSSION

3.1 Study of oxidation of hydrazine by cyclic voltammetry (CV) on ZnO-H, ZnO-O and ZnO-D electrodes

The well polished gold electrodes are coated with ZnO-H, ZnO-O and ZnO-D materials and current response is studied using cyclic voltammetry for a known concentration of hydrazine (33 µM). CV is recorded using these electrode as working electrodes,platinum strip as

counter electrode and Ag/AgCl as reference electrode in 0.02 M PBS (pH = 7.4) in the potential range from - 0.3 to + 0.8 V (Fig. 1). On comparison of the current response of the electrodes, the ZnO-D electrode/ Au is least (1.2 µA) and over potential is highest (0.49 V). The current response for ZnO-O/Au electrode is highest (3.4 µA), the peak is significantly sharper and the over potential is considerably lower (0.25 V). Where as that of ZnO-H stands in between these two with respect to both current and over

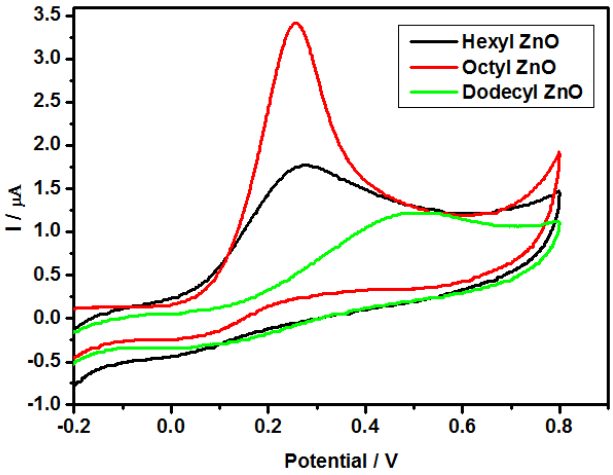

Fig.1. The current response for 33 µM hydrazine on various electrodes using 0.2 M PBS.

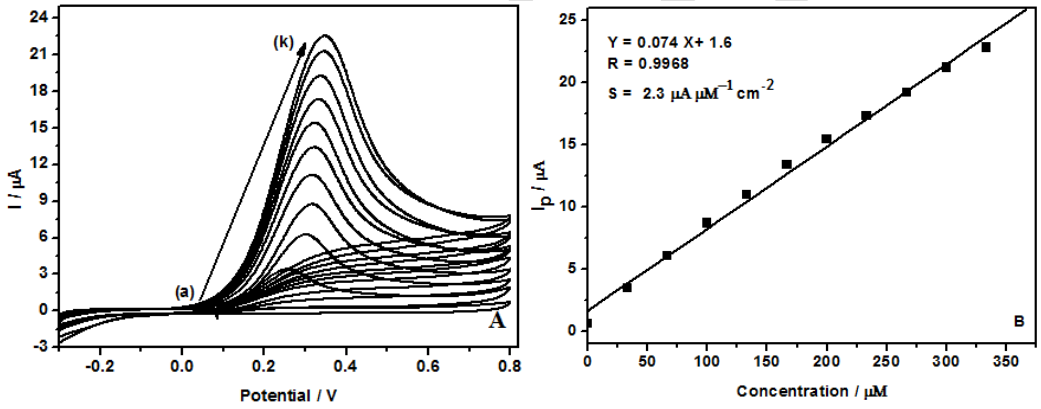

Fig.2 (A) Typical Cyclic voltammogramms for different concentrations of hydrazine ranging from 0 to 333 µM (a to k) in 0.02 M PBS on ZnO-O/Au electrode and (B) The plot for I_p vs. concentration of hydrazine.

3.2 Effect of concentration of hydrazine by cyclic voltammetry on ZnO-O/Au electrode

Fig.2A depicts typical irreversible cyclic voltammogramms of hydrazine oxidation on ZnO-O/Au for different concentrations ranging from 0 to 333 µM, (curves a to k) with 0.02 M PBS at pH 7.4 as supporting electrolyte at a scan rate of 100 mVs^{-1}. The oxidation peak current increases with the increase in the concentration of hydrazine. The cyclic voltammogram in absence of hydrazine is a flat curve. The corresponding peak potential varies from 260 to 350 mV. The peaks are sharper compared

to oxidation current peaks on bare gold electrode (ref). This indicates faster electron transfer in case of ZnO-O/Au electrode. And the plot of $I_p$vs. concentration is found to be linear, (Fig.2B) with a correlation coefficient of R = 0.9958. From the slope of the curve, the sensitivity is found to be equal to 2.3 µA μM^{-1} cm^{-2}, whereas on the bare gold electrode it is 0.85 µA μM^{-1} cm^{-2}. Thus there is an almost three fold increase in current on the ZnO-O/Au electrode.

3.3 Effect of scan rate

Cyclic voltammetry was performed at different scan rates at 1 mM concentration of hydrazine, Fig. 3A. From the plot (Fig.3B, curve a) of I_p vs. $v^{1/2}$, one can find the total number of electrons involved in the electrochemical reaction. The peak current against the square root of potential scan rate shows linear plot indicating the reaction is diffusion controlled. The plot (Fig.3B, curve b) of normalized current, $I_p/v^{1/2}$ vs. scan rate (v) shows the characteristic shape typical of an electro catalytic processes.

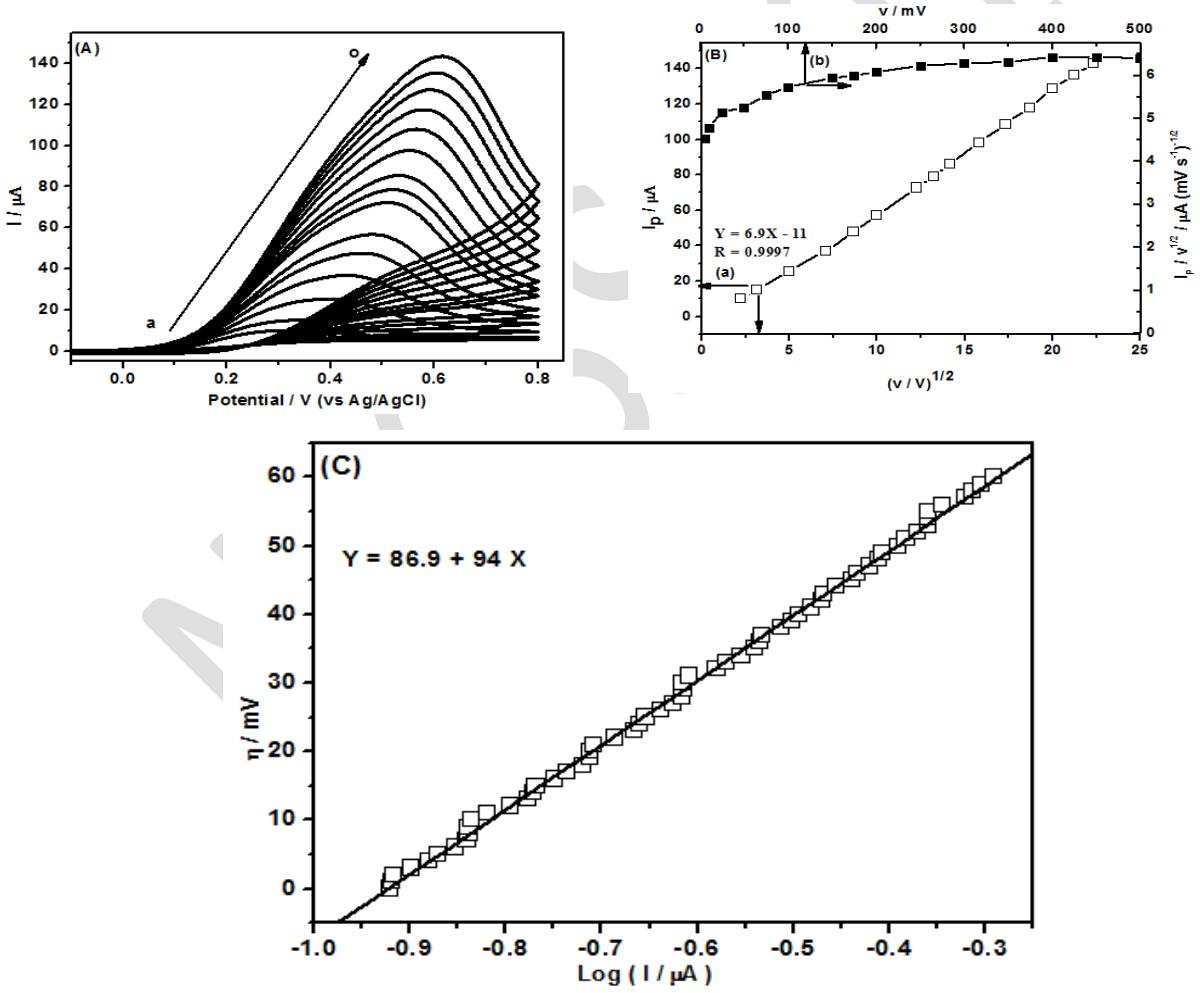

Fig.3 (A) Typical plots at various potential scan rates (5, 10, 25, 50, 75, 100, 150, 175, 200, 250, 300, 350, 400, 450, 500 mVs^{-1}) for a 1 mM concentration of hydrazine using CV, (B) curve (a) The plot of I_p against the square route of potential scan rate, curve (b) the plot of normalized current, $I_p/v^{1/2}$ vs.

scan rate (v), (C) A plot of log I vs. the over potential, η from the rising part of cyclic voltammogram at 5 mVs^{-1} scan rate for 1mM concentration of hydrazine on ZnO-O/Au electrode in 0.02 M PBS.

According to Randles-Sevick equation, for an irreversible processs

We have,

$I_p = 2.99 \times 10^5 n (\alpha n_\alpha)^{1/2} A c D^{1/2} v^{1/2}$ .....(i)

Where I_p is peak current density at a given scan rate for that particular concentration,n and n_α is the total number of electrons and number of electrons in the rate determining step respectively, α is the transfer coefficient, v is the scan rate, c is the concentration of hydrazine in mol/cc and D is the diffusion coefficient. The total number of electrons obtained from the slope of I_p vs. $v^{1/2}$ is 3.9 approximately equal to 4. Considering $\alpha n_\alpha = 0.23$, $D = 1.5\times10^{-4}$ cm^2 s^{-1}, A= 0.0314 cm^{-2}, $c = 1\times10^{-6}$ moles/cm^3. D is obtained from chronocoulometry.

3.4The Tafel like plot

The Tafel like plot obtained from the rising part of the current - voltage curve at 5 mVs^{-1} scan rate using Eq. (ii) yields a Tafel slope of 87 mV/decade (Fig.3 A)

$\log I = \log I_o + (\alpha nF/ 2.303RT) \eta$ ..... (ii)

where η is the over potential.

Transfer coefficient α

From the following equation (Bard),

$(E_p - E_{p/2}) = 48/ \alpha n_\alpha$ …… (iii)

where, E_p and $E_{p/2}$ are peak potential and half peak wave potential respectively at a given scan rate. The value of Transfer coefficient α obtained is equal to 0.23

Based on the above results, the oxidation of hydrazine at 7.4 pH can be considered to under go the following steps.

$N_2H_4 + H_2O \rightarrow N_2H_5^+ + OH^-$ (fast)

$N_2H_5^+ \rightarrow N_2H_3 + 2H^+ + e^-$ (slow)

$N_2H_3 + 3\ H_2O \rightarrow N_2 + 6H^+ + 3OH^- + 3\ e^-$(fast)

It shows that one electron process is the rate determining step followed by three electron process with the evolution of N_2 as the final product.

3.5 Chronocoulometry

One can obtain diffusion coefficient from chronocoulometry and by Cottrell equation,

$$Q = 2nFAc\, D^{1/2}\, \pi^{-1/2}\, t^{1/2} \quad \text{.....(vi)}$$

Where 'n' is the total number of electrons, 'A' is the area of the electrode, 'c' is the concentration of hydrazine in mol/cc, F= 96485 C mol^{-1}. A step potential between - 0.01 and +0.4 V with 500 ms pulse width is setup. Fig.4 A depicts the chronoamperogramms in the absence of hydrazine (a) and in presence of (b) 33, (c) 66, (d) 99, (e)133, (f)166, (g)196, (h) 228, (i) 259 and (j) 333 µM hydrazine in 0.02 M PBS. From the slopes of Q vs. $t^{1/2}$ plots (Fig.4 B), assuming number of electrons 'n' involved in the hydrazine oxidation to be equal to four, the mean diffusion coefficient D is calculated to be equal to 1.5×10^{-4} cm^2 s^{-1}.

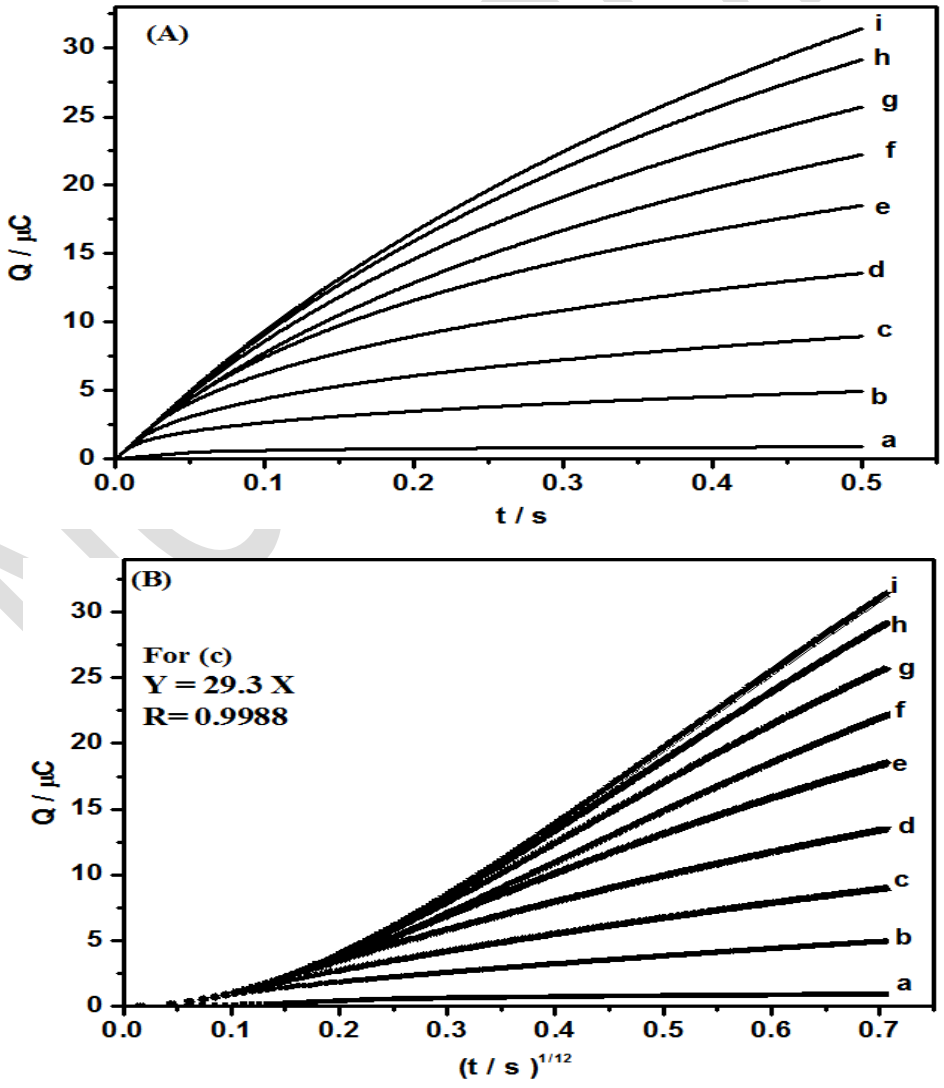

Fig.4. (A) A typical plot of Q vs. t, (B) Q vs. $t^{1/2}$ plots using chronocoulometry for different concentrations (a to i), (0, 33, 66, 99, 133, 166, 199, 233 and 266 µM) of hydrazine in 0.02 M PBS by setting the step potential from - 0.01 and +0.4 V for a 500 ms pulse width on ZnO-O/Au electrode.

3.6 Linear range, Sensitivity and Detection limit by Amperometry

To determine the detection limit and linear range of hydrazine, the ZnO-O/Au electrode is tested for the amperometric detection of hydrazine at an applied potential of +0.3 V in a magnetically stirred phosphate buffer solution 0.02 M (pH 7.4). Upon successive addition of known concentration of hydrazine (3.3 - 322 µM) at intervals of hundred seconds, a typical amperometric response is obtained (Fig.5A). The determined sensitivity is found to be 1.5 µA μM^{-1} cm^{-2} in a linear range from 0.033 to 322 µM with a correlation coefficient R = 0.9955, Fig.5 B.

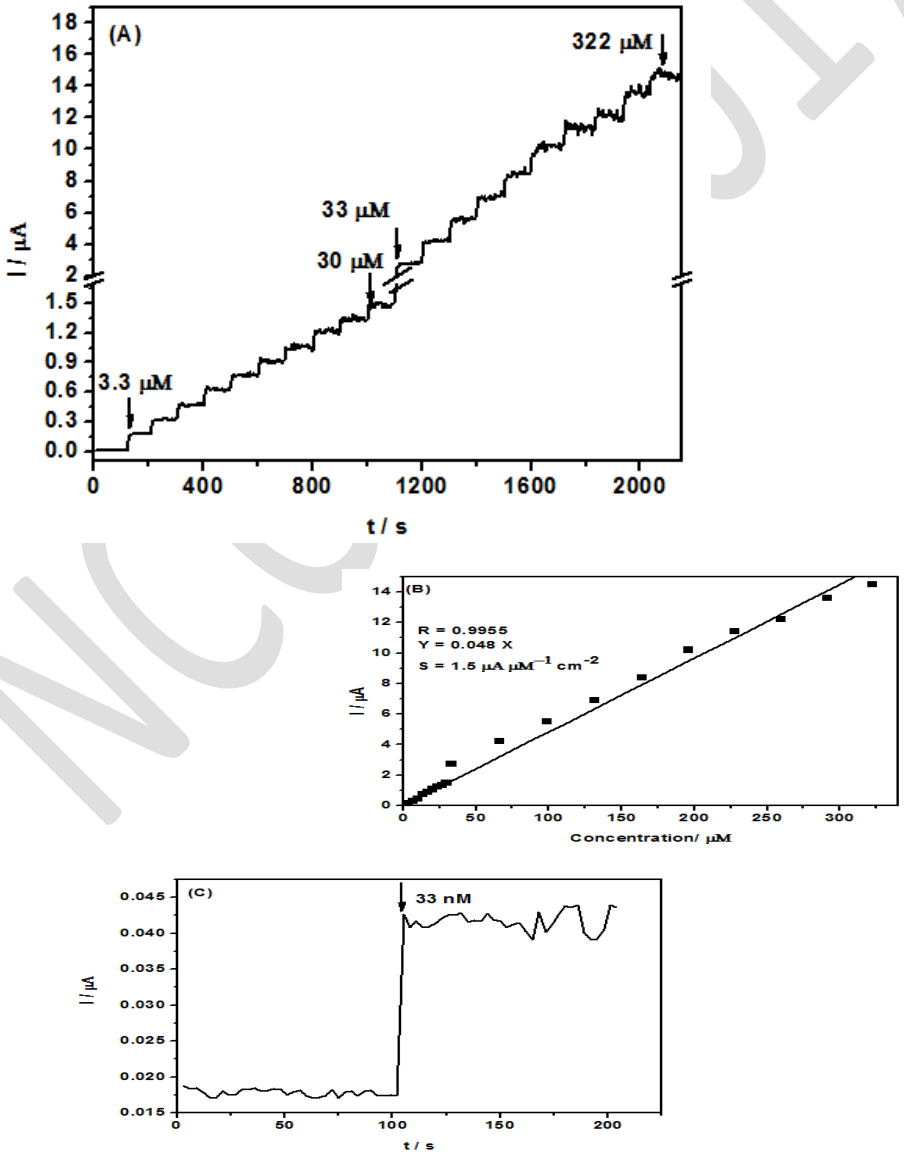

Fig.5 (A) A typical amperogram on addition of 3.3 µM to 322 µM of hydrazine on the ZnO-O/Au electrode in 0.02 M PBS (B) the corresponding linear plot of current vs. hydrazine concentration and (C) Amperogram showing the detection limit of 33 nM.

In order to find the detection limit,hydrazine solution is serially diluted and is injected into the cell containing PBS. Detection limit of 33 nM with the signal to noise ratio of 5, with a response time < 3 seconds is obtained , Fig.5 C. Five replicates of the sample yields a RSD of 2.7.

3.7 Interference study

To test the selectivity of the oxidation of hydrazine, various substances, which are potential interferants are added to the PBS. Cations and anions such as K^{2+}, Mg^{2+}, Ca^{2+}, Cu^{+}, SO_4^{2-}, NO_3^{2-}, urea and glucose (10 fold) in the oxidation of 6.6 µM hydrazine shows less than 3% deviation (Fig.6). This suggests that the ZnO-O/Au electrode is an efficient sensor for hydrazine oxidation.

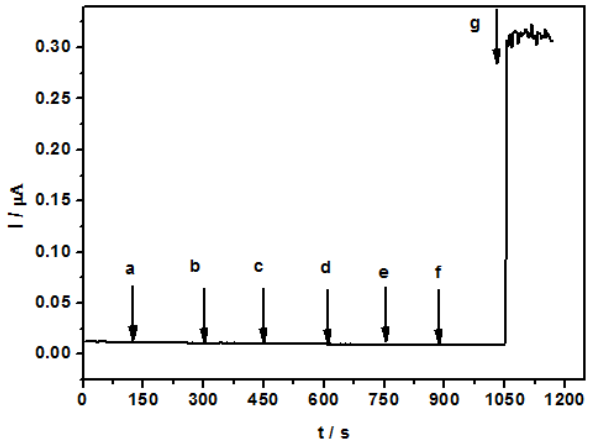

Fig.6. Amperometric current response for 6.6 µM hydrazine on ZnO-O/Au electrode in 0.02 M PBS, in presenceof (a) calcium nitrate, (b) sodium sulphate, (c) cupric nitrate,(d) magnesium nitrate, (e) urea, (f) glucose and (g) hydrazine.(The concentrationsof these compounds are ten fold more than the concentration ofhydrazine).

3.8 CONCLUSION

Zinc oxide prepared earlier using amines of different chain lengths was used to prepare electrodes. Zinc oxide synthesized using octylamine (ZnO-O) showed best electrochemical response for the

detection of hydrazine and is attributed to the quasi one dimensional morphology of ZnO. The ZnO-O/Au electrode showed a very low detection limit of 33 nM with linearity for a wide concentration range (33.0 $x10^{-3}$ µM – 322 µM). The sensitivity of the electrode is found to be 1.5 µA $µM^{-1}$ cm^{-2}. No interference with common cations or anions is observed.

References:

[1] Sultana W, Eraiah B. and Ghosh S, Electroanalysis, 2012, 24, 1869-1877.

[2] Y. Shen, Q. Xu, H. Gao, N. Zhu, Electrochemistry Communications, 2009, 11, 1329.

[3] V. Rosca, M.T.M. Koper, Electrochimica Acta, 2008, 53, 5199.

[4] J. Liu,Y, Li,J, Jiang, X, Huang,Dalton Trans., 2010, 39, 8693.

[5] A. Umar, M.M. Rahman, Y.B. Hahn, Talanta, 2009,77, 1376.

[6] Rafiq A, Nirmalya T, Min-Sang A, Yoon-Bong H, Materials & Design, 2016,109, 530-538

[7] Adel A. I, Farid A. H, M. Faisal, El-Toni.A.M, Al-Assiri M.S., Materials & Design,2016,109.530-538.

[8] Jie Hu, Zhenting Zhao, Yongjiao Sun, Ying Wang, Kun Lian, Applied Surface Science, 2016, 364, 434-441

[9] Mehta S.K, Singh.K, Umar .A, Chaudhary G.R., Singh .S, Electrochimica Acta, 2012, 69, 128-133.

[10] Sultana W, Chethana B.K, Eraiah.B, International J ChemTech Research, 2014, 6, 2141-2143

[11] Sultana W, Eraiah.B, Journal of Chemical Engineering and Research, 2014, 2, 193-199

POSTER PRESENTATIONS

P_01: Stability of the Anatase Phase in Nanodimensional Titanium Dioxide Doped With Eu^{3+}

*Mohamed Zikriya[1], Nadaf.Y.F[2] and Renuka C.G[1]**

[1]Dept. of Physics, Bangalore University, Bengaluru-560056.

[2]Dept. of Physics and Research Centre, Maharani's Science College for women, Bengaluru-560001.

**Corresponding author E-mail:renubub@gmail.com*

ABSTRACT

Titanium dioxide (TiO_2) nanomaterials are attracting increasing interest, mostly because of their superior photocatalytic and antibacterial properties. In this work, we report the synthesized the pure and TiO_2:Eu^{3+} by hydrothermal method, the structural and morphological properties of TiO_2 and TiO_2:Eu^{3+} powder, were studied over a calcinations temperature range of 400 ^{0}C to 800 ^{0}C for 4hours. The structural and morphological characterization was carried out by X-ray diffraction (XRD), Fourier transform infrared (FT-IR) spectrophotometer, Scanning electron microscopy (SEM). The structural crystalline domain shape and size distribution of the synthesis powders were studied by means of X-ray techniques for pure TiO_2 and Eu^{3+} doped presents similar structural characteristics and its phase transformation from the anatase to the rutile confirms at 800 ^{0}C. It was determined that the anatase phase of TiO_2 is stabilized when doped with Eu^{3+}, even at temperatures up to 800 ^{0}C. The XRD pattern of Eu-doped TiO_2 indicated tetragonal crystal structure the average crystallite size was determine by sherrer formula found 8 nm at 400 ^{0}C and 29 nm at 800 ^{0}C. It was observed that the particles consist of nano-sized crystals for all working conditions. Hydrothermal method allowed the successful incorporation of Eu^{3+} ions into the TiO_2 host lattice, and morphological characterization was carried out by SEM, the Eu^{3+} doped sample did not show any commendable morphological change when compared with the pure TiO_2 sample common particle size distribution of each pure and Eu^{3+} doped sample turned into found to be inside the range of 10 nm - 35 nm. It is similar result to the value calculated from XRD analysis. From the picture of SEM the particles are also include nano agglomerates.

Key words: Titanium dioxide, hydrothermal method, tetragonal crystal and crystallite size.

Acknowledgement

The authors are grateful to the DST (SERB) New Delhi for providing financial support through major project No.SR/S2/CMP/-0069/2012. Thanks to Prof. Sharath Ananthamurthy, Coordinator DST-PURSE Programme for Raman characterization at Department of Physics, Bangalore University, Bengaluru.

P_02: Growth and characterization of Zn^{+2} mixed cadmium oxalate crystals

Nagaraja K P[1], Lokannath N K[2] Jagannatha N[1], Susheela K Lenkennavar[1]& Delma D' Souza[1]*

[1]Dept. of Physics, FMKMC College Madikeri, Kodagu District, Karnataka- 571201

[2]Dept. of studies in Physics, University of Mysore, Manasagangothri, Mysuru -570006

E-mail:[1]nagarajkodip@gmail.com *[2]lokanath@physics.uni-mysore.ac.in[1]jagannathnettar@yahoo.co.in

ABSTRACT

Chromium mixed cadmium oxalate crystal (CdZn) is grown by gel diffusion method in silica hydro gel by varying gel parameters such as specific gravity, p^H and gel aging, concentration of reactants and varying ratio of mixture Cd to Zn. The optimum conditions for the crystal growth are established. Cation such as Zn^{+2} is used to replace some intrinsically available Cd^{+2} ions in the lattice of mixed cadmium oxalate crystals. Occupation of Zn ions in the lattices of few Cd ions have changed the morphology of original cadmium oxalate crystals, results the growth of new mixed CdZn crystals. The mixed cadmium oxalate crystals were characterized using energy dispersive X-ray spectroscopy (EDAX) and thermo-gravimetric analysis (TGA). FTIR analysis of the mixed CdZn crystals is carried out to know the functional groups. Optical properties and electrical conductivity of grown crystals are measured. Results obtained for mixed CdZn crystals are compared with that of intrinsic cadmium oxalate crystals. Depending on their properties, the oxalate mixed crystals will be used in the development of special semiconducting devices.

Key words: Mixed crystal, Cation, Cadmium oxalate, CdZn, Conductivity

P_03: Molecular conformation and packing features in a series of aryl substituted tetrahydropyrimidine-5-carboxylates

Vasu,[a] Deepak Chopra,[b] T. N. Guru Row[c]

a: Government First Grade College, Kengeri Bangalore 560 060
c: Indian Institute of Science Education and Research, Govindpura, Bhopal 462023.
c: Solid State and Structural Chemistry Unit, IISc., Bangalore5-60012.

ABSTRACT

Pyrimidines derivatives are medicinally important compounds possessing antitumour , antiviral and cardiovascular agents Atwal (1989). The compound 2-thiopyrimidine shows a pronounced "in-vitro" bacteriostatic activity Holy et al., (1974). Literature survey reveals that dihydro pyrimidines (DHPM) possess potent calcium blocking activity and diverse range of biological activity Kappe (1993).

Thus there has been considerable interest in the chemistry, molecular geometry and the probable biological activity of the compound is a prerequisite for any understanding of its potent pharmacological properties

In view of this, supramolecular structures of eight tetrahydropyrimidine-5-carboxylates derivatives were analyzed in order to understand the effect of variations in functional groups on molecular geometry, conformation and packing of molecules in the crystalline lattice. It is observed that the existence of an intra-molecular C-H…π interaction between the aromatic hydrogen with the isolated double bond is a key feature which imparts stability to the molecular conformation. The compounds pack *via* the involvement of N-H…S=C and N-H…O=C intermolecular dimers forming a sheet like structure in the solid state.

e-mail : vasusriranga@rediffmail,com

Mobile: 9901079879

P_04: Studying effect of carrier fluid viscosity in magnetite based ferrofluids using optical tweezers

*Savitha S.[1#], Shruthi S. Iyengar[1], Sharath Ananthamurthy[1] and Sarbari Bhattacharya[1]**

[1] Department of Physics, Bangalore University, Bangalore, Karnataka, INDIA.
[#] Department of Physics, Government First Grade College, Chickballapura, Karnataka, INDIA.

**Email: sarbari.bhattacharya@bub.ernet.in*

ABSTRACT

Ferrofluids are magnetic fluids that exhibit normal fluid like behavior with superparamagnetic properties. Ferrofluids are basically suspensions of magnetic nanoparticles in a suitable carrier liquid. The magnetic nanoparticles are coated with suitable surfactants to prevent agglomeration. The nanoparticles involved are superparamagnetic in nature possessing a single magnetic domain and exhibit negligible retentivity and coercivity. The viscosity of ferrofluids is greatly influenced by external magnetic fields. These unusual properties of ferrofluids make them potential candidates for various industrial and biomedical applications.

Ferrofluids with varying viscosities of carrier fluids have been prepared with magnetite (Fe_3O_4) nanoparticles. The nanoparticles were synthesized by chemical co-precipitation and characterized by X-Ray Diffraction (XRD) and Field Emission Scanning Electron Microscopy. They were found to be nearly spherical in shape with an almost uniform size of 13nm.The superparamagnetic nature of the water based ferrofluids at room temperature is established by SQUID magnetometry. Dynamic light scattering (DLS) was carried out to establish the size of the nanoparticle clusters in the ferrofluids synthesized. The results indicate an increase in cluster size with increase in carrier fluid viscosity. This is supported by results from Raman Spectroscopy. A further attempt to characterise these ferrofluids was made by studying the behaviour of well characterised non-magnetic micron sized probes that are optically trapped while suspended in the ferrofluid. An increase in carrier fluid viscosity results in a decrease in corner frequency when only the carrier fluid is used as the suspending medium. When the magnetic component is also present the corner frequency is higher than with just the carrier fluid. This relative increase happens at all laser powers at the trapping plane. This trend is also found to be independent of the size and material of the probe particle. Comparison of various parameters that influence optical trapping leads us to believe that the enhancement could be due to a directed motion of the magnetic clusters in the presence of an optical trap.

Keywords: ferrofluid; carrier fluids; viscosity; optical tweezers.

P_05: Long Monitoring Spectroscopic study of MRK509 with IUE Satellite

Vedavathi P* and Vijayakumar H Doddamani*,

Dept. of Physics, Bangalore University, Bangalore-560056,

Email-ID:drvkdmani@gmail.com, M: 09448673274

ABSTRACT

IUE satellite has made long monitoring UV spectroscopic observations of a few Seyfert 1 galaxies, BL Lac Objects and Quasars. Active galaxies as a special class of galaxies are characterized by high continuum and line luminosity variability over a wide range of time-scales. The time-scales and the amplitude of variability can used to probe the geometrical sizes of broad line regions surrounding the central compact nuclei in these exotic objects. The long monitoring studies of active galaxies are useful in understanding the physical process responsible for continuum and line variabilites observed in most of the active galaxies. In this Paper, We present our studies on MRK509, a Quasar / Seyfert 1 galaxy observed with IUE satellite over 15years. We have found a good linear correlation between the fluxes of strong UV lines such as Lyα, Si IV, C IV, C III] and MgII lines with the underlying UV continuum. We observed high amplitude flux variations in Lyα than compared to Si IV line. These results are in a general agreement with the predictions of photo-ionization model.

Keywords: active galaxies, super massive black holes, accretion processes, low redshift,

P_06: Nanosecond Nonlinear Optical Properties of Sodium Triborate Glasses doped with Gold Nanoparticles

G Jagannath [1], B Eraiah [1], R Rajaramakrishna [2]*

[1] Department of Physics, Bangalore University, Bangalore-560056, Karnataka, India.

[2] Department of Physics, National College, Jayanagar, Bangalore-560070, Karnataka, India.

E-mail: eraiah@rediffmail.com

ABSTRACT

Nonlinear optical properties of gold nanoparticles (NPs) doped Sodium triborate glasses have been investigated using open aperture Z-scan technique with 532 nm nanosecond pulses. Sodium triborate glasses synthesized from melt quench method were characterized by Uv-Vis absorption, Z-scan and HR-TEM measurements. Uv-Vis spectra of undoped glasses does not showed any absorption peak whereas glasses doped with gold NPs presents a broad SPR band of Au NPs at ~582 nm due to interband transition. HR-TEM image confirms the presence of Au NPs with a particle size ranging from 8 nm to 45 nm and an average particle size of 25 nm. It has been observed that, gold NPs doped glasses showed reverse saturable absorption (RSA) kind of nonlinearity under nanosecond pulse excitation due to interband transition from d-band to the conduction band within Au NPs. The Z-scan results revealed that, the studied glasses are potential candidates for optical limiting devices.

P_07: A study on changing weather patterns in Bengaluru

Ananya D, R Rajaramakrishna[*]

The National College, Jayanagar, Bengaluru

ABSTRACT

The climate in Bengaluru is having a lot of variations in the last decade. It is experiencing an urban heat island effect, heat waves, deluges that resemble cloudbursts and changes in other climatic factors within the city limits that differ from its surroundings. The city is also experiencing varied precipitation and there are changes in micro-climate as well. It becomes essential to study and make analysis about these changes as it has a direct impact on the city's environment and its living conditions.

For a land-locked region like Bengaluru, variations in rain patterns and extreme hot and cold periods are the indicators of extreme weather. A faster rise in average minimum temperature is being observed, as well as the average maximum temperature reaching its peak since the last year.

This might be described as a localized impact of the climate change. But predominantly, it seems like the rapid population growth, coupled with an increase in different kinds of pollution, especially air and water is accelerating these changes. Also, decrease in water evaporation and transpiration leads to conditions like heat island. This in turn has an influence on the other weather parameters as well. An overview of the condition indicates that these variations in the weather patterns not only become more frequent, but it might get more intense. Hence, it becomes important to consider the weather data and study its variations over the years. Automatic Weather Monitoring System (AWS) developed by ISRO plays a key role in this process. AWS records data of the hourly changes in the various weather parameters like temperature, atmospheric pressure, wind speed and direction, rainfall, relative humidity and solar radiation. The sensors used in the AWS helps in recording data with precision and track small changes in the weather, thereby increasing the reliability of surface observations. Using the metadata, statistical interpretation of the various plots is made to study the weather patterns. Plots like average rainfall and average maximum and minimum temperature over the years helps in analyzing the variation in them. This might further be used to understand the causes for the same and future implications if any. In this article, I would like to emphasis on the change in weather patterns in Jayanagar locality of Bengaluru. A detailed insight on atmospheric parameters such as temperature, rainfall, humidity and pressure is monitored. The data from Automatic Weather Monitoring System installed in The National College, Jayanagar, obtained for an area of radius 10 square kilometers is considered for the same.

[*]E-mail: r.rajaramakrishna@gmail.com

P_08: Induced Polystyrene effects on removal of natural polymer in Mangifera Indica

Anil Kumar.S, Chaithanya.K.N, Dhanalakshmi.M, Soundharya.S.V, Thontadharya Deekshith.M, Thejas.R, Siddalingeshwara.B.P, [*]

Department of PG studies and research in physics, The National College, Jayanagar Bangalore-560070

[*]E-mail:siddu.nandi143@gmail.com

ABSTRACT

Lignin is a complex organic polymer deposited in a cell walls of many plants, making them rigid and woody. It is a polymer consisting of various aromatic alcohols, and the chief non-carbohydrate constituent of wood. The Mangifera Indica was subjected to lignin removal solution and then replaced with POT. The IR studies on these samples infers that the polymer doped sample was more hardened as the ratio of peak confirms the sample is more prone towards hard wood, which has a range of applications in construction of buildings and architectural designs. The moisture absorption and decomposition rate of two different samples were performed. The relative moisture absorption was calculated and tabulated to establish the respective absorption co-efficient.

Key words: Mangifera Indica, Lignin, Polystyrene, IR Spectra, DTA, Moisture test.

P_09: Diurnal variations of Atmospheric Electric Field at Mysuru (12°*N*), India.

Pruthvi Rani K. S., Pranamya M.P., Kempaiah A. and Chandrashekara M. S.[*]

Department of Studies in Physics, University of Mysore, Manasagangotri, Mysuru, India
[*]msc@physics.uni-mysore.ac.in

ABSTRACT

The atmosphere, vital to terrestrial life, is the gaseous envelope surrounding the Earth. The Earth's atmosphere is continually electrified. Our understanding of the global atmospheric electrical circuit, which is the global circuital path which links the lower troposphere, the ionosphere and the magnetosphere, has improved since the discovery of electric field in the early twentieth Century, although this area of geophysics still provides both theoretical and experimental scientific challenges. The simultaneous measurement of Electric field, temperature and humidity parameters of the atmosphere provides an ideal topic for educational outreach in environmental science. The variability of the electric field measured at the surface is attributed to meteorological sources, both global and local in origin. By investigating the variability in electrical parameters under different atmospheric conditions, these global and local sources can be separated. As a consequence, information on global thunderstorm and shower cloud activity can be retrieved, which is of direct relevance to research on global climate change.

The atmospheric electric field is measured using a Field Mill at Manasagangotri, Mysuru during fair weather days of 2015-2016. The Field Mill is an instrument used for the study of vertical electric field in the atmosphere by several researchers. Meteorological parameters such as temperature, relative humidity, atmospheric pressure, wind speed and wind direction were simultaneously recorded using AWS. Atmospheric electric field varied from 78.7 $V\ m^{-1}$to 226.31 $V\ m^{-1}$with an average of 129.46 $V\ m^{-1}$. The diurnal variation of atmospheric electric field is compared with the standard Carnegie curve and the data appears to follow the trend of the Carnegie curve. The atmospheric electric field in the Carnegie curve was found to increase gradually from 04 hours to 20 hours. Whereas at Mysuru station the field is found to be almost constant from 04 to 14 hours with lower values and there was a sharp increase from 14 hours to 20 hours. The deviations from the standard curve may be due to local influence of afternoon convective mixing, typical of land stations. Maximum value of atmospheric electric field is observed in the night 19 hours and minimum value is observed during night at 23 hours.

P_10: Effect of Strontium on Li_2O-V_2O_5-B_2O_3 conducting glasses

Anagha Rao[1], Divya K S[1], Hemanth Kumar S[1], Rajaramakrishna[1,]*

[1] Department of Post Graduate Studies & Research in Physics, The National College, Jayanagar, Bangalore – 560070.

*Corresponding author: [*r.rajaramakrishna@gmail.com](mailto:r.rajaramakrishna@gmail.com)*

ABSTRACT

Strontium doped Lithium Vanadium Borate glasses were prepared using the conventional quench technique. AC conductivity of these glasses as a function of frequency have been carried out at various temperatures, where the conductivity ranges from $1.05X10^{-9}$-$1.18X10^{-7}$S/m. The symmetric and asymmetric structural network of these glass samples were studied using Infrared (IR) and Raman Spectroscopic techniques. IR measurements were done over a spectral range 400-1700 cm^{-1}, where all absorption bands above 500 cm^{-1} correspond to borate network. The Raman spectra were recorded over the range 200-2000cm^{-1}, which confirmed the borate units in the glass samples. The glass transition temperature (T_g) was studied using Differential Scanning Calorimetry (DSC), with a programmed heating rate of 1^0/min in the temperature range 30 - 550^0C, where the T_g is found to be in the range 415 – 445^0C.

Keywords: Conducting glasses, Borate glasses, IR Spectra, Raman Spectra, DSC

P_11: Chemical Synthesis of Chromium Oxide nano powders

*Yathish Kumar, Naveen Kumar T. R., Vinay Prasad, Rajanna. N. G. Pramod**

Department of Post Graduate (Physics), The National College (Autonomous), Jayanagar, Bangalore-560070

ABSTRACT

Cr_2O_3nano powders were prepared using Chromium Chloride asprecursor material, NaOH and distilled water as solvents. Two different samples of 0.1M and 0.2M were synthesized and they weresubjected to an annealing temperature from 200˚-500˚C.The samples were characterized by X-ray diffraction (XRD) for their structural analysis andvarious parameters viz., lattice constants, strain, etc. have beenestimated.It has found that unannealed samples exhibit pure amorphousnature as no peak is observed in the XRD pattern.All the annealed samples show sharp crystalline peaks with well-defined FWHM values.We conclude that heat treatment of the samplesaugments the crystallinity of the sample.

Keywords: Chromium Oxide, Nano particles, chemical synthesis, heat treatment

Corresponding Author: Tel.: +91-90352 84380
e-mail: pramodng@gmail.com

P_12: Crystal and Molecular docking studies of biscyclohexane diol with focal adhesion kinase inhibitors

K S Kiran[1, 2], M K Kokila[2], Guruprasad R[3]*

[1] Department of physics, School of Engineering and Technology, Jain University, Bangalore, Karnataka, India*

[2] Department of physics, Bangalore University, Bangalore, Karnataka, India

[3] Scientific Director, Durga Femto Technologies & Research, Bangalore, Karnataka, India

*****Corresponding author
Email: kiranxrd@gmail.com

ABSTRACT

In the present study crystal structure of 3-hydroxy-2-((2-hydroxy-4, 4-dimethyl-6-oxocyclohex-1-enyl) (4-methoxyphenyl) methyl)-5, 5-dimethylcyclohex-2-enonewas determined using single crystal X-ray diffraction. Cyclohexane is a non planar molecule the shape of which vaguely resembles a chair. The conformation of cyclohexane molecule is constantly changing, with the atom on the left which is currently pointing down flipping up, and the one on the right flipping down. Further the structural feature was extrapolated to molecular docking studies with focal adhesion kinase (FAK) domain using Autodock to study its anticancerous property. The compound exhibited considerable bacterial inhibition of lower to moderate concentrations. We conclude that these derivatives can be used in medicine and have enormous potential as pharmaceutical agents due to their biological activities. The above titled receptor gain functional and structural insights into their mechanism of inhibition and explore its potential as an anticancer agent.

Keywords: Bis cyclohexyl diols, Docking, Focal adhesion kinase, anticancer therapy target.

References:

(1)Wallace, A. C.; Laskowski, R. A.; Thornton, J. M. Protein Engineering 1995, 8, 127-134.

(2).Sureshbabu, N.; Sughanya, V. Acta Crystallographica Section E 2012, 68, o2638.

(3).Huang, D.; Cheung, A. T.; Parsons, J. T.; Bryer-Ash, M. Journal of Biological Chemistry 2002, 277, 18151- 18160.

(4) O'Boyle, N. M.; Banck, M.; James, C. A.; Morley, C.; Vandermeersch, T.; Hutchison, G. R. Journal of Cheminformatics 2011, 3, 33-33.

P_13: Physical and Optical Properties of Copper doped Lanthanum Strontium Borate Glasses

Thontadharyadeekshith.M[1], Rojashree.S[1],Suraj.K[1], Abhiram.J[1],R.Rajaramakrishna[1*], Rajashekara K M[2]*

[1]Department of Post Graduate and Research in Physics, The National College Jayanagar, Bangalore

[2]Department of Physics, S.J.C.I.T., Chikkaballapura

ABSTRACT

The glass composition of $10La_2O_3$-30SrO-$60B_2O_3$-xCuO, where x = 0, 0.1, 0.2, 0.5 and 1 (in mole %) has been synthesized by the conventional melt quench technique. The powder X-Ray diffraction analysis of the prepared samples confirms the amorphous nature of the samples. Density measurements for these glasses were done and physical parameters were studied. Structural properties of these glasses were analyzed through infrared spectra that were recorded between 1600cm^{-1} and 400cm^{-1} in transmission mode. The optical band gap for the glasses was obtained from plots between $h\nu$against$(\alpha h\nu)^2$ and$(\alpha h\nu)^{\frac{1}{2}}$. The value of Band gap were found to be around 2.8 to 3eV, by extrapolating the straight line tangent to the energy axis the optical band gap for these glasses were measured. IR reveals the existence of various borate segments above 500 cm^{-1}. An absorption peak at lower wave number like 520 -560 $cm^{-1}$is witnessed for Sr^{2+}.

Key words: Optical Band gap, Copper doped glasses, Urbach Energy

***Corresponding author:**

r.rajaramakrishna@gmail.com
abhi.ram.jagan@gmail.com

P_14: Effective electron densities and effective atomic numbers of brass, solder lead and steel wool for gamma irradiation.

S. Prasanna Kumar[1] and T. K. Umesh[2]

[1]JSS Academy of Technical Education, Bangalore 560060, India
[2] DOS in Physics, University of Mysore, Manasagangotri, Mysore 570006, India
E-mail: spkjss@gmail.com

ABSTRACT

The Effective atomic number and effective electron densities of Brass, Solder lead and Steel wool in the gamma energy range 280keV to 1115keV are determined on a goniometer assembly [1]. An ORTEC model 23210 gamma-x high purity germanium detector (HpGe) has been used to record the data along with a personal computer based MCA in the angular region 50^0-110^0. The results, the effective atomic number Z_{eff} and the effective electron densities N_{eff}, so obtained are of first of their kind at these energies and are expected to play a vital role in the variety of applications of Radiation Physics, Condensed matter Physics, Space Sciences and so on.

P_15: Growth and Characterization of Amorphous Nickel Oxide thin films by SILAR Method

*Abhishek P., Prajwala A. R., Ranjitha A. P, N. G. Pramod**

Department of Post Graduate (Physics), The National College Jayanagar (Autonomous), Bangalore-560070

ABSTRACT

This work presents a chemical route for the preparation of NiO thin films on glass substrates. A simple and inexpensive Successive Ionic Layer Adsorption and Reaction (SILAR) technique was employed to deposit NiO thin films using $NiCl_2.6H_2O$ as the precursor and Sodium Hydroxide (NaOH), Distilled Water as solvents. Three different samples 0.1M, 0.15M and 0.2M were grown. Some of these samples were annealed and the change in the properties of annealed with respect to un-annealed samples were studied. Structural characterization by XRD reveals the films to be amorphous in nature. Surface morphology of the films has been studied by Atomic Force Microscopy (AFM) and the samples show clear presence of coalesced grains. Heat treatment makes the sample surface smoother and this is seen in the surface roughness values. Further, the samples were characterized optically by UV-Visible spectroscopy and various optical properties viz., Transmittance and Band Gap of the film samples were estimated. We find that the value of the optical transmittance gradually reduces as the molarity of the samples increases. Conversely, the direct band gap has been found to vary proportionally with molarity.

Keywords: SILAR, Nickel Oxide, Thin films, characterization

Corresponding author: Tel.: +91- 90352 84380

E-mail: pramodng@gmail.com

P_16: Energy and Environment

V. S Veena

Department of Physics, Government First Grade College, Madhugiri, Karnataka
Email id:veenapradeep10@gmail.com,
Mobile.no:9591736814

ABSTRACT

Energy use and supply is of fundamental importance to society and, with the possible exception of agriculture and forestry, has made the greatest impact on the environment of any human activity - a result of the large scale and pervasive nature of energy related activities. A major aim of Energy and Environment is to act as a forum for constructive and professional debate between scientists and technologists, social scientists and economists from academia, government and the energy industries on energy and environment issues in both a national and international context. It is also the aim to include the informed and environmentally concerned public and their organizations in the debate. Particular attention is given to ways of resolving conflict in the energy and environment field.

Energy and Environment is an interdisciplinary theme at natural scientists, technologists and the international social science and policy communities covering the direct and indirect environmental impacts of energy acquisition, transport, production and use. A particular objective is to cover the social, economic and political dimensions of such issues at local, national and international level. The technological and scientific aspects of energy and environment questions including energy conservation, and the interaction of energy forms and systems with the physical environment, are covered, including the relationship of such questions to wider economic and socio-political issues. Papers covering energy related aspects of wider environmental questions are included, such as the use of fuel wood and continuing impacts of de-forestation and their importance.

ISSN 2394-5710